Lawrence Berkeley National Laboratory

Title

Drought Shifts Sorghum Root Metabolite and Microbiome Profiles and Enriches for Pipecolic Acid

Permalink

https://escholarship.org/uc/item/6311z544

Journal

Phytobiomes Journal, 7(4)

ISSN

2471-2906

Authors

Caddell, Daniel F

Pettinga, Dean

Louie, Katherine

et al.

Publication Date

2023-12-01

DOI

10.1094/pbiomes-02-23-0011-r

Copyright Information

Peer reviewed

OPEN ACCESS

phytobiomesjournal.org APS

Phytobiomes Journal

A Transdisciplinary Journal of Sustainable Plant Productivity

RESEARCH

Drought Shifts Sorghum Root Metabolite and Microbiome Profiles and Enriches for Pipecolic Acid

Daniel F. Caddell,[1,2] Dean Pettinga,[2] Katherine Louie,[3,4] Benjamin P. Bowen,[3,4] Julie A. Sievert,[5] Joy Hollingsworth,[5] Rebeckah Rubanowitz,[2] Jeffery Dahlberg,[5] Elizabeth Purdom,[6] Trent Northen,[3,4] and Devin Coleman-Derr[1,2,†]

[1] Plant Gene Expression Center, U.S. Department of Agriculture-Agricultural Research Service, Albany, CA 94710
[2] Plant and Microbial Biology Department, University of California Berkeley, Berkeley, CA 94720
[3] Lawrence Berkeley National Laboratory, Berkeley, CA 94720
[4] DOE Joint Genome Institute, Lawrence Berkeley National Laboratory, Berkeley, CA 94720
[5] Kearney Agricultural Research and Extension Center, Parlier, CA 93648
[6] Department of Statistics, University of California Berkeley, Berkeley, CA 94720

ABSTRACT

Plant-associated microbial communities shift in composition as a result of environmental perturbations, such as drought. It has been shown that Actinobacteria are enriched in plant roots and rhizospheres during drought stress. However, the correlations between microbiome dynamics and plant response to drought are poorly understood. Here we apply a combination of bacterial community composition analysis and plant metabolite profiling in *Sorghum bicolor* roots, rhizospheres, and soil during drought and drought recovery to investigate potential contributions of host metabolism to shifts in bacterial composition. Our results provide a detailed view of metabolic shifts across the plant root during drought and show that the response to rewatering differs between root and soil; additionally, we identify drought-responsive metabolites that are highly correlated with the observed changes in Actinobacteria abundance. Furthermore, we find that pipecolic acid is a drought-enriched metabolite in sorghum roots, and that exogenous application of pipecolic acid inhibits root growth. Finally, we show that this activity functions independent of the systemic acquired resistance pathway and has the potential to impact Actinobacterial taxa within the root microbiome.

Keywords: 16S rRNA, amplicon sequencing, drought, metabolomics, microbiome, pipecolic acid, roots, sorghum

By taking advantage of advances in high-throughput sequencing technologies, researchers are beginning to understand the dynamic nature of the root microbiome. For instance, it is known that microbiomes vary between environments (Bulgarelli et al. 2012; Lundberg et al. 2012; Peiffer et al. 2013), between species

(Fitzpatrick et al. 2018; Naylor et al. 2017; Ofek-Lalzar et al. 2014), and even between varietals of the same species (Edwards et al. 2015; Haney et al. 2015; Peiffer et al. 2013; Walitang et al. 2018). Additionally, microbiomes shift with developmental age, particularly as the plant transitions between vegetative and reproductive growth (Chaparro et al. 2014; Edwards et al. 2018; Xu et al. 2018). It has been shown that the root microbiome also responds to abiotic stresses; for example, during drought, the plant root exhibits enrichment in Gram-positive bacteria, and especially Actinobacteria. This phenomenon has been corroborated across diverse plant clades (Fitzpatrick et al. 2018; Naylor et al. 2017; Santos-Medellín et al. 2017; Xu et al. 2018), and it has been hypothesized that these changes may improve plant fitness under drought (Fitzpatrick et al. 2018). While there is interest in using such knowledge to engineer crop microbiomes for enhanced plant growth during drought stress, more research is needed to understand the timeline of these changes and what role the plant plays in shaping this response.

Interestingly, it has been observed that while Gram-positive bacteria become dominant in the root microbiome during drought, their enrichment may be transitory, with Gram-negative bacteria

eventually being reestablished after rewatering (Xu et al. 2018). This resilience in the root microbiome may suggest that plants directly or indirectly mediate these shifts (Koyama et al. 2018; Simmons et al. 2020) through transient changes in plant signaling or metabolism. Under nondrought conditions, plant-derived metabolites have been predicted to drive the community structure of the microbiome, as changes in exudation patterns between photoperiods (Baraniya et al. 2018) and across development (Chaparro et al. 2013, 2014; Zhalnina et al. 2018) both track changes in the microbiome. A recent study of the maize leaf microbiome across 300 maize genotypes observed associations between specific microbial taxa and host metabolic functions (Wallace et al. 2018), and other studies have shown that different combinations of root exudates are sufficient to alter microbiome composition (Badri et al. 2013), likely by impacting chemotaxis and behavior of soil microbes (Huang et al. 2019; Zhang et al. 2014). Some of these plant-produced metabolites may act as carbon sources for microbes (Cai et al. 2009), while others may act to repel specific taxa (Bressan et al. 2009; Hu et al. 2018; Huang et al. 2019; Iven et al. 2012; Wang et al. 2013, 2018c). Despite its potential importance in shaping the microbiome, the role of root metabolic dynamics during drought and its correlation with observed shifts in Gram-positive and Gram-negative dominance has not been explored extensively. Currently there is considerable interest in developing microbiome-based products to improve drought tolerance in crops; gaining a better understanding of the relationship between root metabolomics during environmental perturbation and microbiome recruitment and assembly will facilitate the rational design of microbiome-based products and predictable outcomes for their application.

In this study, we utilize a preflowering drought treatment applied to field-grown sorghum to explore changes in root metabolism and their correlation with enrichment in Gram-positive bacteria during drought and the transition back to Gram-negative dominance following rewatering. Toward this goal, we employed 16S rRNA amplicon sequencing and metabolomic profiling of roots, rhizosphere, and soil at the peak of drought and 24 h after rewatering. As anticipated, we observe enrichment in Gram-positive bacteria during drought (Fitzpatrick et al. 2018; Naylor et al. 2017; Xu et al. 2018) and demonstrate that the microbiome responds rapidly to rewatering in a compartment-specific manner. We also discover that drought alters the metabolite profiles of sorghum roots, rhizospheres, and soils, and that known drought-associated metabolites such as betaine, 4-aminobutanoic acid (GABA), and proline exhibit distinct enrichment patterns across compartments and time. Notably, the abundance of a large number of rhizosphere metabolites is rapidly depleted by rewatering following drought, whereas few metabolites shift abundance in the root during this time frame. In addition to other better-known drought-associated metabolites, we report drought-induced enrichment in pipecolic acid (Pip), a lysine catabolite that has been identified as an essential component of systemic acquired resistance (SAR) (Bernsdorff et al. 2016; Návarová et al. 2012), but with additional suspected roles in abiotic stress response (Arruda and Barreto 2020). Here, we demonstrate that exogenous application of Pip has the ability to suppress plant root growth, a phenomenon often observed during plant physiological response to drought. Finally, we show that this activity functions independent of the established SAR pathway and may play a role in modulating root microbiome dynamics during drought stress.

MATERIALS AND METHODS

Field experimental design and sample collection. Sorghum cultivar 'RTx430' plants were grown in the summer of 2017, in a field located at the UC-ANR KARE Center located in Parlier, California (36.6008°N, 119.5109°W), as described previously by Gao et al. (2020) and Xu et al. (2018). Sorghum seeds were sown into prewatered fields. Starting in the third week, control treatment plants were watered 1 h three times per week by drip irrigation (1.89 liter/h flow rate), and no water was provided to drought treatment plants. After 8 weeks, which coincided with the average onset of flowering across all plants, root and rhizosphere samples were harvested from a subset of field samples prior to watering (TP8). Crop water stress indices, indicating severity of drought stress experienced by sorghum under this experimental design, were calculated and published in Xu et al. (2021). Water was then restored to the drought plots (rewatered), and root and rhizosphere samples were harvested after 24 h (TP8 + 24 h). All field samples were collected between 11 a.m. and 12 p.m. using a modified version of the protocol described in detail in Simmons et al. (2018). Soil samples were collected using a 15-cm soil core sampler, approximately 20 cm from the base of the plant. To collect rhizosphere compatible with both microbiome and metabolomic analyses, excavated plants were briefly shaken to dislodge excess soil, and an ethanol-sterilized nylon-bristled toothbrush was used to remove closely adhering soil from the root, which we collected as the rhizosphere fraction, prior to vortexing the roots twice for 1 min in epiphyte removal buffer (ice-cold 0.75% KH_2PO_4, 0.95% K_2HPO_4, 1% Triton X-100 in ddH_2O; filter sterilized at 0.2 μm with Corning brand filters). Any remaining soil adhering to the root was separated with epiphyte removal buffer and discarded. The roots were again rinsed with clean epiphyte removal buffer and patted dry. All samples were immediately flash-frozen in LN_2 in the field and stored at –80°C until sample processing.

Microbox experimental design. Sorghum cultivar RTx430 seeds were surface-sterilized, and then they imbibed in Petri dishes containing autoclaved filter paper and Milli-Q water in the dark at 30°C for 24 h. Four seeds each were sown into 1.3 kg of field soil from UC-ANR KARE that was prewetted with 130 ml of autoclaved $1/2\times$ Murashige and Skoog media (pH 5.8) with or without 1 mM pipecolic acid in 12 square Microbox containers (TP5000 + TPD5000, SacO2, Dienze, Belgium) and maintained in a growth chamber (28/22°C, 16 h day, $\sim$250 μmol $m^{-2}s^{-1}$). Five days later, half of the seedlings were subjected to a drought treatment by setting Microboxes in laminar flow hoods overnight, with the lids open (drought) or closed (watered). This process was repeated for an additional night, after which droughted leaves had visible leaf curling and the Microboxes had lost $\sim$1 kg of weight. Droughted and watered Microboxes were returned to the growth chamber for 7 days, after which plant roots and tightly associated rhizospheres were harvested and immediately flash-frozen in LN_2 and stored at –80°C until sample processing. Measurements of shoot length and shoot fresh weight of each plant were taken at the same time as root sampling.

DNA extraction, amplification, and amplicon sequencing. DNA extraction was performed using the protocol for collection of root endosphere, rhizosphere, and soil samples using a Qiagen DNeasy Powersoil DNA extraction kit with 0.15 g (roots) and 0.25 g (rhizosphere and soil) as starting material in the provided collection vials, as described in detail in Simmons et al. (2018). The V3-V4 region of the 16S rRNA gene was PCR amplified from 25 ng of genomic DNA using dual-indexed 16S rRNA Illumina iTags 341F (5′-CCTACGGGNBGCASCAG-3′) and 785R (5′-GACTACNVGGGTATCTAATCC-3′). Barcoded 16S rRNA amplicons were quantified using a Qubit dsDNA HS assay kit on a Qubit 3.0 fluorometer (Invitrogen, Carlsbad, CA), pooled in equimolar concentrations, purified using Agencourt AMPure XP magnetic beads (Beckman Coulter, Indianapolis, IN), quantified using a Qubit dsDNA HS assay kit on a Qubit 3.0 fluorometer

(Invitrogen), and diluted to 10 nM in 30 µl total volume before being submitted to the QB3 Vincent J. Coates Genomics Sequencing Laboratory facility at the University of California, Berkeley for sequencing using Illumina Miseq 300 bp pair-end with v3 chemistry.

Amplicon sequence processing and analysis for field experiment. 16S amplicon sequencing reads were demultiplexed in QIIME2 (Bolyen et al. 2019) and then passed to DADA2 (Callahan et al. 2016) to generate amplicon sequence variants (ASVs), with taxonomies assigned using the August 2013 version of GreenGenes 16S rRNA gene database as described previously (Simmons et al. 2020). All subsequent 16S statistical analyses were performed in R-v3.6.1 (R Core Team 2021). To account for differences in sequencing read depth across samples, samples were normalized by dividing the reads per ASV in a sample by the sum of usable reads in that sample, resulting in a table of relative abundance frequencies, which were used for analyses, with the exception of alpha-diversity calculations, for which all samples were normalized to an even read depth of 29,918 ASVs per sample. Alpha diversity was determined with the *estimate_richness* function in the R package phyloseq-v1.30.0 (McMurdie and Holmes 2013), and significance was tested by ANOVA using the *aov* function in the R stats package. Beta diversity (PCoA) was performed using the *ordinate* function in the R package phyloseq-v1.30.0 (McMurdie and Holmes 2013). Sample type separation was determined by pairwise PERMANOVA with 1,000 permutations using the *adonis* and *calc_pairwise_permanovas* functions in the R packages vegan-v2.5.6 (Dixon 2003) and mctoolsr-v0.1.1.2. Tukey-HSD tests used the *HSD.test* function in the R package Agricolae-v1.3.1. The combined metabolite and bacterial ASV heatmaps were generated using the R package pheatmap-v1.0.12.

Metabolite extraction and LC-MS. In preparation for metabolomics, root tissue was ground with a mortar and pestle containing LN_2. Root water content was estimated by lyophilizing root tissue and calculating the difference between wet and dry weights. Root samples were then normalized so that the lightest sample was 0.2 g (wet weight) and each other sample was at least 0.2 g. Rhizosphere and soil water contents were estimated to obtain similar amounts of material. The overall difference in % water content between samples was minimal (2.5 to 6.5%). For extraction of polar metabolites from ground root tissue (0.2 to 0.3 g wet weight), samples were first lyophilized dry, and then 500 µl of methanol was added, followed by a brief vortex and sonication in a water bath for 10 min. Samples were centrifuged for 5 min at 5,000 rpm and then supernatant was transferred to 2-ml tubes and dried in a Speed-Vac (SPD111V, Thermo Scientific, Waltham, MA), and extracts were stored at –80°C. For soil and rhizosphere samples (1.25 g wet weight), polar metabolites were extracted similarly, but samples were not lyophilized prior to extraction, 2 ml of LC-MS grade water was added, followed by vortex and water bath sonication for 30 min and centrifugation for 7 min at 7,000 rpm, and then supernatant was transferred to a 5-ml tube, frozen, and lyophilized dry, and extracts were stored at –80°C.

In preparation for LC-MS, tissue, soil, and rhizosphere extracts were resuspended with 300 µl of methanol containing internal standards (~15 µM average of 5 to 50 µM of 13C,15N Cell Free Amino Acid Mixture; 5 µg/ml 4-(3,3-dimethyl-ureido)benzoic acid (#CDS014672, Sigma); 5 µg/ml 3,6-dihydroxy-4-methylpyridazine (#668141, Sigma); 9 µg/ml d5-benzoic acid (#217158, Sigma); 1.3 µg/ml 9-anthracene carboxylic acid (#A89405, Sigma); 10 µg/ml 13C-trehalose (#TRE-002, Omicron); 10 µg/ml 13C-mannitol (#ALD-030, Omicron). Samples were vortexed and sonicated 10 min, centrifuged 5 min at 5,000 rpm, and supernatant centrifuge-filtered 2.5 min at 2,500 rpm (0.22 µm hydrophilic PVDF, Millipore, Ultrafree-CL GV, #UFC40GV0S), and then

150 µl was transferred to LC-MS glass autosampler vials. Root extracts were resuspended similarly, but with resuspension volume varied to normalize by root dry weight.

Chromatography was performed using an Agilent 1,290 LC stack, with MS and MS/MS data collected using a Thermo QExactive Orbitrap MS (Thermo Scientific, Waltham, MA). Full MS spectra were collected from *m/z* 70 to 1,050 at 70,000 resolution in both positive and negative ion modes, with MS/MS fragmentation data acquired using stepped 10, 20, and 40 eV collision energies at 17,500 resolution. Mass spectrometer source settings included sheath gas flow rate of 55 au (arbitrary units), auxiliary gas flow of 20 au, spray voltage of 3 kV (for both positive and negative ionization modes), and capillary temperature of 400°C. Chromatography was performed using a HILIC column (Agilent InfinityLab Poroshell 120 HILIC-Z, 2.1 × 150 mm, 2.7 µm, #673775-924) at a flow rate of 0.45 ml/min with a 2-µl injection volume. To detect metabolites, samples were run on the HILIC column at 40°C equilibrated with 100% buffer B (95:5 ACN/H_2O with 5 mM ammonium acetate) for 1 min, diluting buffer B down to 89% with buffer A (100% H_2O with 5 mM ammonium acetate and 5 µM methylenediphosphonic acid) over 10 min, down to 70% B over 4.75 min, then down to 20% B over 0.5 min, followed by isocratic elution in 80% buffer A for 2.25 min. Samples consisted of three biological replicates each and three extraction controls, with sample injection order randomized and an injection blank (2 µl of MeOH) run between samples.

Metabolite identification and analysis. Metabolite identification was based on exact mass and comparison of retention time (RT) and MS/MS fragmentation spectra to those of standards run using the same chromatography and MS/MS method. Custom Python code (Yao et al. 2015) was used to analyze LC-MS data. For each feature detected (unique *m/z* coupled with RT), a score (0 to 3) was assigned representing the level of confidence in the metabolite identification. Positive identification of a metabolite had detected $m/z \leq 5$ parts per million (ppm) or 0.001 Da from theoretical as well as $RT \leq 0.5$ min compared with a pure standard run using the same LC-MS method. The highest level of positive identification (score of 3) for a metabolite also had matching MS/MS fragmentation spectra compared with either an outside database (METLIN; Smith et al. 2005) or an internal database generated from standards run and collected on a QExactive HF Orbitrap MS. Identifications were invalidated if MS/MS from the sample mismatched that of the standard. MS/MS mirror plots for metabolites are presented in Supplementary Materials.

Totals of 112 and 122 polar metabolites were identified in positive and negative ion modes, respectively (Supplementary Table S1). If a metabolite was observed in both ion modes, the mode with higher peak height was selected for the merged metabolite profile ($n = 168$) used for all analyses. Values below the limit of detection were imputed with the lowest observed values in the dataset rounded down (2,400 or 1,900 for positive or negative ion modes, respectively; Supplementary Table S2). Principal components analysis of metabolite profiles was performed using the *prcomp* function in the R stats package. Venn diagram construction utilized Venny-v2.1.0 (Oliveros 2007-2015). We clustered microbial ASV abundances and metabolite data as has been done previously to detect correlations between these distinct features of host–microbiome systems (Korenblum et al. 2020; McHardy et al. 2013; Roux et al. 2022; Wang et al. 2023). Clustering was performed using the *pheatmap* function in R (Kolde 2019) with scaling based on matrix-wide *z*-scores. All other metabolite analyses were performed using MetaboAnalyst-v4.0 (Chong et al. 2018, 2019). Heatmaps were generated using Euclidean distance and Ward clustering algorithms. We evaluated enriched or depleted

metabolites with the cutoffs of $\log_2$ fold change greater than 2 or less than -2, and a P value of less than 0.05.

Plant root growth assays. Sterilized seeds of the sorghum cultivar RTx430 were germinated on Petri dishes with autoclaved Milli-Q water or autoclaved Milli-Q water containing the defined concentration of Pip overnight in the dark at 28°C, before being transferred to a growth chamber (28/22°C, 16-h day, ppf $\sim$250 μmol m^{-2}s^{-1}). The *Arabidopsis* ecotype Columbia (Col-0) was used in this study. Mutant lines *fmo-1* (SALK_026163; Mishina and Zeier 2006), *npr1-1* (CS3726; Cao et al. 1997), *rbohd/rbohf* (CS68522; Torres et al. 2002), and *azi1-2* (SALK_085727; Jung et al. 2009) were obtained from the Arabidopsis Biological Resource Center (Lamesch et al. 2012). Sterilized seeds were grown on MS plates containing 1/2$\times$ Murashige and Skoog salt mix, 1% sucrose (pH 5.8), 0.8% agar, and the defined concentration of Pip. Use of 1 mM pipecolic acid as a maximum value in our experiments (we included 0.1 mM as well) is consistent with other recent experiments conducted in plants for root assays (Wang et al. 2018a) and leaf assays (Chen et al. 2018). Plants were first stratified for 3 days at 4°C before being transferred to a growth chamber (21°C, 16-h day, ppf $\sim$120 μmol m^{-2}s^{-1}). Root lengths were measured using ImageJ-v1.52a software (Schneider et al. 2012). ANOVA was performed using the *aov* function in the R stats package and Tukey-HSD tests used the *HSD.test* function in the R package Agricolae-v1.3.1. The SAR pathway image was created with BioRender.com.

Amplicon sequence processing and analysis for microbox experiment. 16S amplicon sequencing reads were demultiplexed in QIIME2 (Bolyen et al. 2019) and then passed to DADA2 (Callahan et al. 2016) to generate ASVs, with taxonomies assigned using the SILVA 138 rRNA gene database (Quast et al. 2013) as described by Simmons et al. (2020). All subsequent 16S statistical analyses were performed in R-v4.0.2 (R Core Team 2021). To account for differences in sequencing read depth across samples, samples were normalized by dividing the reads per ASV in a sample by the sum of usable reads in that sample, resulting in a table of relative abundance frequencies, which were used for analyses. Beta diversity analyses: PCoA and constrained analysis of principal components (CAP) were performed using the ordinate function in the R package phyloseq-v1.34.0 (McMurdie and Holmes 2013). Sample type separation was determined by pairwise PERMANOVA with 1,000 permutations using the *adonis* and *calc_pairwise_permanovas* functions in the R packages vegan-v2.5.6 (Dixon 2003) and mctoolsr-v0.1.1.2. Differential abundances of ASVs were determined using the quasi-likelihood F-test framework in edgeR-v-3.32.1 (Robinson et al. 2010).

Microbial growth assays. Seven isolates representing five genera, *Streptomyces, Acinetobacter, Pseudomonas, Chryseobacterium,* and *Bacillus*, were tested for their capacity to metabolize and grow on pipecolic acid as a carbon source. Isolates were streaked from glycerol stocks onto TSB plates. After two days of growth at 30°C, one colony of each isolate was inoculated into 3 ml each of M9: 450 ml of water + 50 ml of 10$\times$ M9 salts (70 g of Na$_2$HPO$_4\cdot$7H$_2$O, 30 g of KH$_2$PO$_4$, 5 g of NaCl, 10 g of NH$_4$Cl) + 1 ml of MgSO$_4$ (1 M) + 50 ml of CaCl$_2$ (1 M), M9 + 1 mM pipecolic acid, and M9 + 0.4% glucose. Tubes were incubated at 30°C and shaken at 250 rpm for 14 days. Growth was measured by OD$_{600}$ with a SmartSpec Plus (Bio-Rad, Hercules, CA) 4, 7, 9, and 14 days postinoculation.

RESULTS

The sorghum root-associated microbiome is influenced by drought and responds rapidly to rewatering. To explore the temporal dynamics of drought stress and rewatering in the microbiome and the metabolome of the root environment, a field experiment was performed in the Central Valley of California. Sorghum plants were either subjected to a prolonged preflowering drought, where no water was applied between planting and the onset of flowering (TP8), or regularly irrigated throughout the experiment (Fig. 1A). To analyze microbiome community changes across these treatments, we performed 16S rRNA community profiling of roots, rhizosphere, and soil using Illumina MiSeq, targeting the V3 to V4 variable regions (Fig. 1B to J). In agreement with a previous study of the sorghum drought microbiome (Xu et al. 2018), which was performed at the same location in a previous year, alpha diversity significantly differed between sample types (Shannon, $F = 82.19$, $P = 1.36 \times 10^{-13}$), with lower diversity in the roots, as compared with rhizosphere and soil, and reduced diversity was observed in droughted roots compared with watered roots (ANOVA, Tukey-HSD, $P < 0.001$; Fig. 1C). Beta diversity was assessed through principal coordinates analysis (PCoA) using Bray–Curtis dissimilarities. The primary axis distinguished samples foremost by compartment (roots, rhizosphere, or soil), and the second axis by watering regime (droughted or well-watered; Fig. 1D), suggesting that both compartment and drought were driving factors shaping the microbiome. Pairwise permutational multivariate analysis of variance (PERMANOVA) was performed for each compartment, each treatment, and the interaction between compartment and treatment, and all were significantly different ($q < 0.05$; Fig. 1D). Similarly to previous studies of root microbiomes, we observed a significant enrichment of Gram-positive bacteria during drought, including taxa belonging to the phylum Actinobacteria in roots and rhizosphere, and Firmicutes in the rhizosphere (ANOVA, Tukey-HSD, $P < 0.05$; Fig. 1B, E, and F). Likewise, Gram-negative lineages were depleted during drought, including Proteobacteria in roots and rhizosphere, Bacteroidetes in roots, and Gemmatimonadetes in the rhizosphere (ANOVA, Tukey-HSD, $P < 0.05$; Fig. 1B and G to I). These results suggest that the sorghum-root-associated microbiome was responsive to drought, in corroboration of past studies.

Following drought, the sorghum root microbiome has been shown to respond to rewatering, with a transition from Gram-positive back to Gram-negative dominance after a 1-week recovery period (Xu et al. 2018). To better understand the early dynamics of this response to rewatering, we watered the droughted sorghum plots after sampling at TP8, and 24 h later performed a second sampling of roots, rhizosphere, and soil. Notably, no significant shifts in relative abundance of root endosphere phyla were observed (Fig. 1B). In this time frame, however, a significant depletion in Actinobacteria and an increase in Gemmatimonadetes occurred in the rhizosphere (ANOVA, Tukey-HSD, $P < 0.05$; Fig. 1B, E, and I). Based on beta diversity, differences between rewatered and drought-stressed rhizosphere microbiomes were easier to visualize than those between rewatered and drought-stressed roots or soils (Fig. 1D). Collectively, these results demonstrate that the rhizosphere environment responds with a more rapid return to Gram-negative dominance than the roots upon rewatering.

Drought alters the metabolite profiles of sorghum roots, rhizosphere, and soil. Zhalnina et al. (2018) determined root metabolome differences across plant age to drive microbe community assembly in the rhizosphere in another Poaceae relative of sorghum, *Avena barbata*. To explore which changes in roots and rhizosphere metabolism during drought correlate with shifts in bacterial community assemblage in field-grown sorghum, we performed an untargeted liquid chromatography–mass spectrometry based metabolomic profiling of roots, rhizosphere, and soil, using the same samples as in bacterial profiling described above. Using a metabolite atlas as reference (Bowen and Northen 2010), 112 and 122 polar metabolites were predicted in positive and

negative ion modes, respectively. When combined, these two lists produced a total of 124 unique metabolites (Supplementary Materials; Supplementary Tables S1 and S2). Within this list of 124 metabolites, we observed different patterns across both compartments and treatments, with individual metabolites that were either drought-enriched or drought-depleted (Fig. 2A) in roots and rhizosphere. To better understand the relationships between samples, a principal component analysis (PCA) was performed; PC1 accounted for 59.5% of the total variation and PC2 accounted for 17.1% of the variation, and overall the plot showed clear separation of samples by both compartment and watering regime (Fig. 2B). Next, we aimed to determine metabolites that were significantly enriched (Log$_2$ fold change > 2, t test P < 0.05) in each compartment during drought. In total, 28, 35, and 16 metabolites were significantly enriched during drought in roots, rhizosphere, and soil, respectively (Supplementary Table S3). Interestingly, approximately half of these enrichments (n = 31; 10 in roots, 13 in rhizosphere, and 8 in soil) were specific to a single compartment; indeed, roots and rhizospheres each showed approximately as many compartment-specific differences (n = 27; 10 in roots and 17 in rhizosphere) as similarities (n = 18; Fig. 2C).

In droughted roots, we observed increases in the relative abundance of many metabolites that are known to respond to abiotic stress, including amino acids, osmoprotectants, antioxidants, hormones, and organic acids (Fig. 2D; Supplementary Table S4), and several distinct patterns of enrichment across the treatment matrix.

Surprisingly, three classically important drought markers, ABA, 1-aminocyclopropane-1-carboxylic acid (1-ACC, the precursor to ethylene), and betaine, exhibited three distinct patterns of drought enrichment across the root and rhizosphere compartments (Fig. 2D). In contrast, only three metabolites were significantly more abundant in watered conditions, including xylitol and the phenolics 2,3-dihydroxybenzoic acid and 4-methylcatechol; these compounds are direct catabolism products of salicylic acid and methylsalicylate, respectively, which are important components of plant immune signaling (Cámara et al. 2007; Zhang et al. 2013; Fig. 2E; Supplementary Table S3). Collectively, these observed metabolite enrichment patterns are consistent with sorghum roots responding metabolically to drought in a compartment-specific manner.

Response to rewatering within 24 h following a prolonged drought varies by compartment. As the sorghum root and rhizosphere microbiomes responded to rewatering differently after 24 h, we next sought to understand whether metabolite profiles would follow a similar compartment-specific trend. Notably, within the first 24-h period, roots were only weakly responsive to rewatering, with no metabolites strongly enriched or depleted (Log$_2$ fold change > 2, t test P < 0.05; Fig. 3A). However, several metabolites were modestly enriched in the root (Log$_2$ fold change > 1, t test P < 0.05), including cytosine, sphinganine, N-acetylglutamic acid, which promotes growth of root hairs and swelling of root tips (Philip-Hollingsworth et al. 1991), and ferulic acid, which is capable of inhibiting root growth and promotes root branching (Caspersen
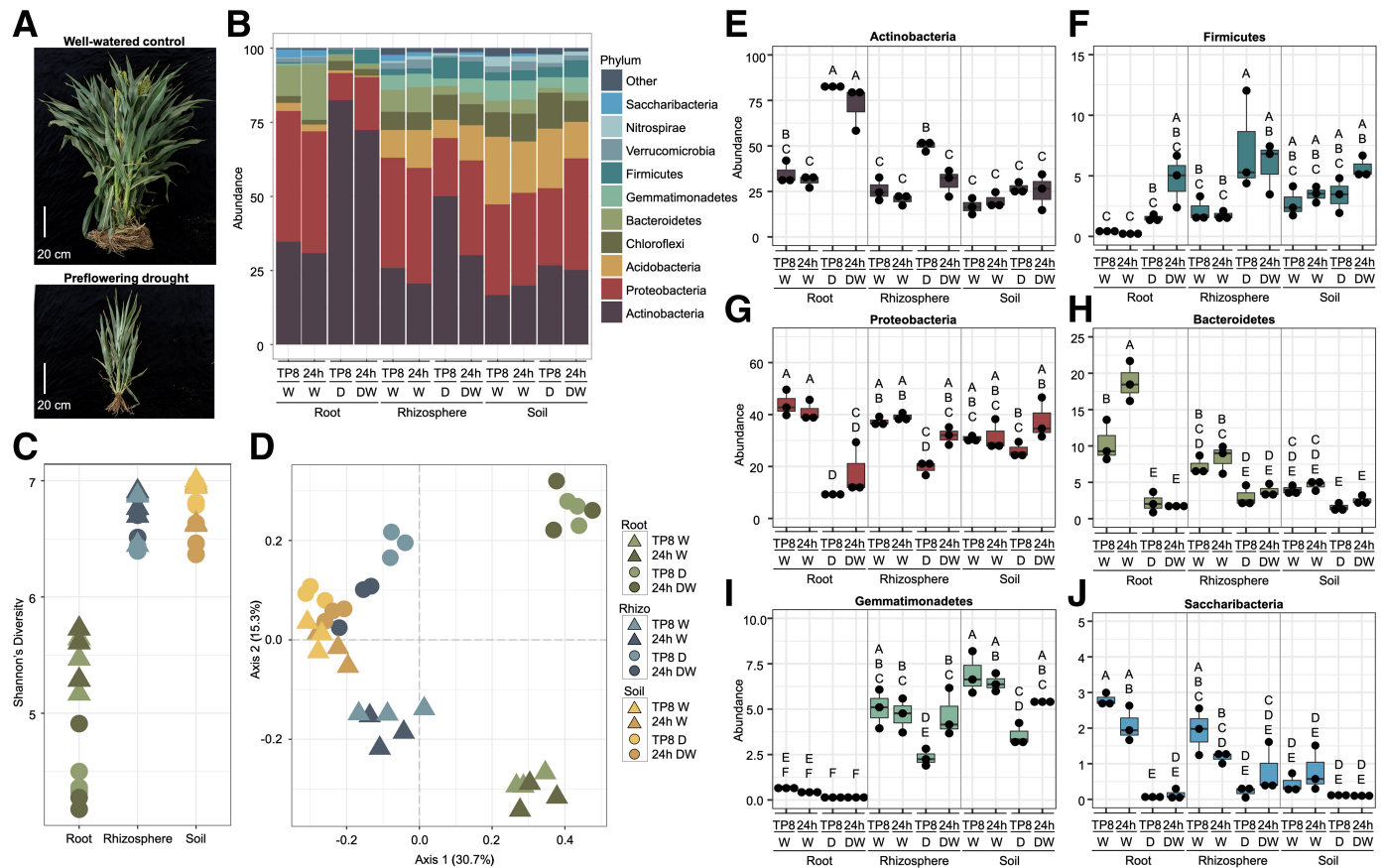

Fig. 1. Sorghum-root-associated microbiome responds to drought and rewatering. **A,** Representative images of a well-watered control sorghum plant and following 8 weeks of preflowering drought (TP8). **B,** Phylum-level relative abundances of sorghum root, rhizosphere, and soil microbiomes at TP8 and 24 h after rewatering (24 h DW) in well-watered (W) or drought (D) plots. **C,** Alpha diversity (Shannon) of sorghum roots, rhizosphere, and soil. **D,** Beta diversity (PCoA) of sorghum root, rhizosphere, and soil microbiomes at TP8 and 24 h after rewatering in well-watered control or drought plots. **E to J,** Relative abundances of individual lineages that displayed a significant difference in abundance between watering treatments (ANOVA, Tukey-HSD, P < 0.05).

et al. 1999; Supplementary Table S5). Collectively, this relatively weak response in metabolism suggests that root endosphere metabolite profiles are largely unchanged within the first day following rewatering.

We hypothesized that while rewatering would eventually shift metabolite compositions across all compartments, the most dramatic and immediate changes would be observable in the rhizosphere, where surface-adhered compounds that accumulated during drought (Fig. 2A) could be flushed away rapidly into the surrounding soil. Consistent with this hypothesis, we observed large shifts in metabolite abundances in the rhizosphere after rewatering, with rewatering tending to cause a depletion of rhizosphere metabolites (Fig. 3A). Significantly depleted metabolites ($n = 17$, Log$_2$ fold change < -2, t test $P < 0.05$) included 10 different organic acids, four sugar alcohols, sn-glycero-3-phosphocholine, carnitine, and melatonin (Fig. 3B; Supplementary Table S6). In contrast, in soils only a single metabolite, trehalose, was significantly depleted following rewatering (Fig. 3C; Supplementary Table S6). Overall, the metabolite composition of the rewatered rhizosphere became more similar to that of watered rhizospheres, but remained distinguishable from all soil profiles (Fig. 3D).

Pipecolic acid suppresses plant root growth. Betaine, an important osmoprotectant, represents one of the most robust and widely utilized biomarkers of plant responses to drought (Caddell et al. 2019; Sakamoto and Murata 2000). We hypothesized that other metabolites with abundance patterns similar to that of betaine may play roles in plant drought response. To identify other putative drought-relevant metabolites, we ranked metabolites based on their correlation coefficients (Pearson's r) with betaine, across all compartments, treatments, and timepoints (Fig. 4A to C). The metabolite most strongly correlated with betaine, pipecolic acid (Pip), is a lysine catabolite that has been identified as a critical component of the SAR pathway (Bernsdorff et al. 2016; Návarová et al. 2012; Fig. 4B and C). It is worth noting that it has also been shown to play a putative but enigmatic role in abiotic stress response in rapeseed (Moulin et al. 2006) and in the halophyte *Triglochin maritima* (Goas et al. 1976). Beyond Pip, the other 9 of the top 10 correlated metabolites have all been identified previously in recent literature as drought-relevant metabolites. These include 4-aminobutanoic acid (GABA) (Bown and Shelp 2016), allantoin (Irani and Todd 2018; Nourimand and Todd 2017), carnitine (Khan et al. 2019; Oney-Birol 2019), and the amino acids proline, tyrosine, asparagine, serine, glutamine, and trans-4-hydroxyproline (Fàbregas and Fernie 2019; Fang and Xiong 2015; Gargallo-Garriga et al. 2018; Rai 2002; Ranieri et al. 1989; Fig. 4A).
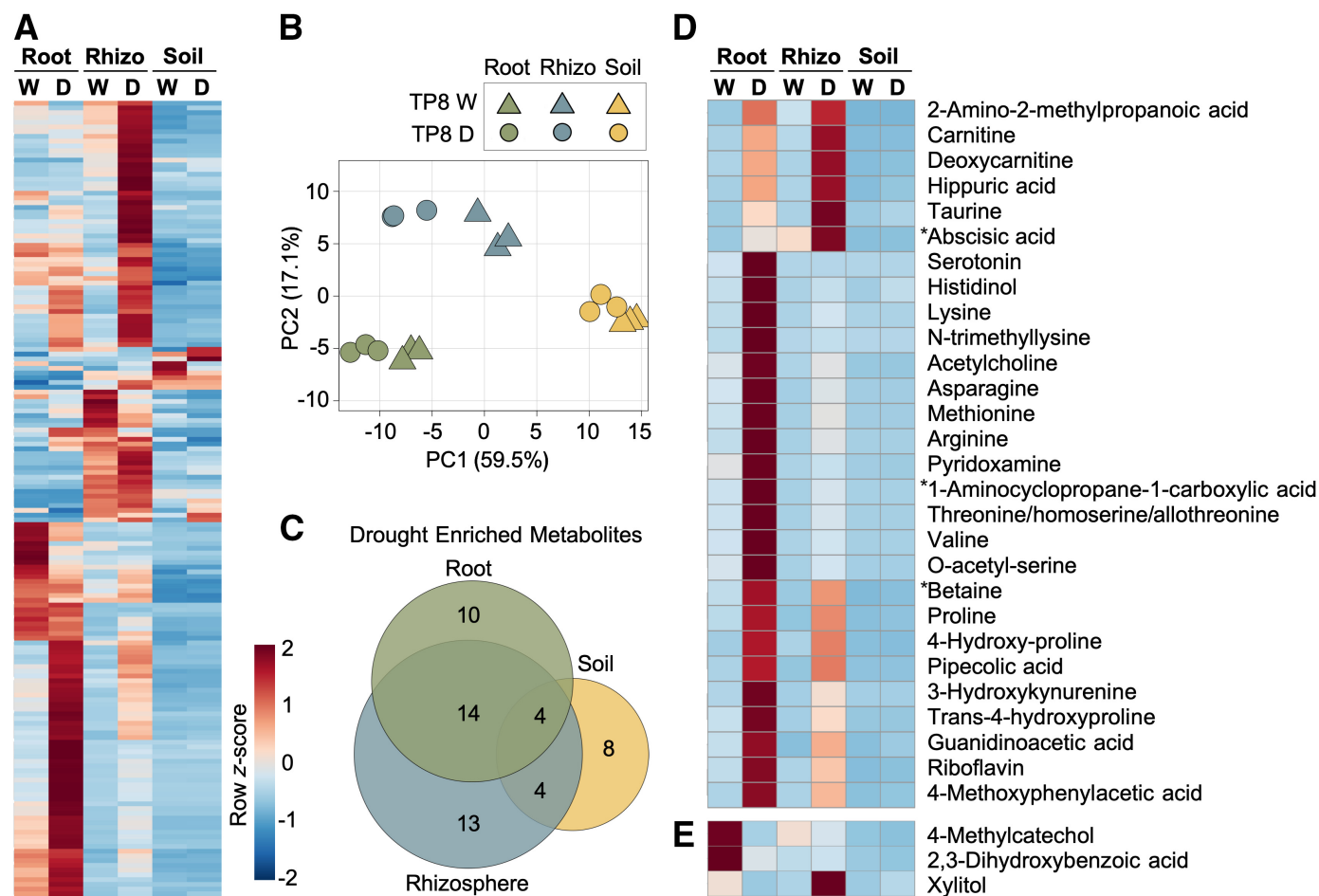

Fig. 2. Metabolic profiles during drought differ by compartment. A, Heat map of relative peak heights of all observed metabolites ($n = 124$) across root, rhizosphere [rhizo], and soil compartments and watered (W) and drought (D) treatments. B, Principal component analysis (PCA) plot of root, rhizosphere, and soil metabolites. C, Proportional Venn diagram of drought-enriched metabolites in roots, rhizosphere, or soil (D/W Log$_2$ fold change > 2, t test $P < 0.05$). D and E, Heat map of the subset of metabolites that were enriched, D, or depleted, E, in roots during drought, with the predicted identity of metabolites listed beside each row. Classical drought markers observed, D, and noted in text are annotated with asterisks. Note that hippuric acid and 3-hydroxykynurenine, which have mainly been studied in mammalian systems, may be misidentified, as their MS/MS mirror plots lacked resolvable isomers (Supplementary Material).

A key goal of this study was to identify potential interactions between these drought-related metabolites and the root-associated bacterial community. To this end, we clustered bacterial ASVs (grouped at the class level) and metabolites based on abundances across all compartments, treatments, and time points (Supplementary Fig. S1). Strikingly, while the majority of metabolites and bacterial classes separated into distinct clusters, three microbial lineages, including the Actinobacteria, nested within a metabolite-dominant node, just adjacent to the metabolite cluster containing the top 10 betaine-correlated metabolites (Fig. 4D). When clustering was performed based solely on the abundances in the root, where host control of the microbiome is anticipated to be strongest (Naylor et al. 2017) and Actinobacteria enrichment under drought is strongest (Xu et al. 2018), we observed that the Actinobacteria formed a close linkage with betaine-correlated metabolites, and was specifically clustered with five metabolites, including pipecolic acid (Fig. 4D and E).

Pipecolic acid and plant drought response. As pipecolic acid is a metabolite that is correlated with Actinobacterial enrichment patterns under drought, and plays an as yet unclear role in drought response in the root, we chose to explore the relationship between pipecolic acid, drought response, and the microbiome further. It has been shown that Pip application leads to reduced root growth in *Arabidopsis* (Wang et al. 2018b); reduced root growth can be caused by many stimuli, but is also a commonly observed phenomenon during drought response (Sebastian et al. 2016; Tsuji et al. 2005). To evaluate whether Pip application provokes a similar response in sorghum, we germinated sorghum in Petri dishes containing water plus 0, 0.1, or 1 mM Pip. Seven days after germination, 1 mM Pip-treated sorghum displayed significantly reduced root growth (Fig. 5A and B); we confirmed that a similar response occurs in *Arabidopsis*. Average root growth was reduced in all Pip treatments in a dosage-dependent manner, with significant decreases in root growth observed with 0.1 and 1 mM Pip concentrations (Fig. 5C and D). These
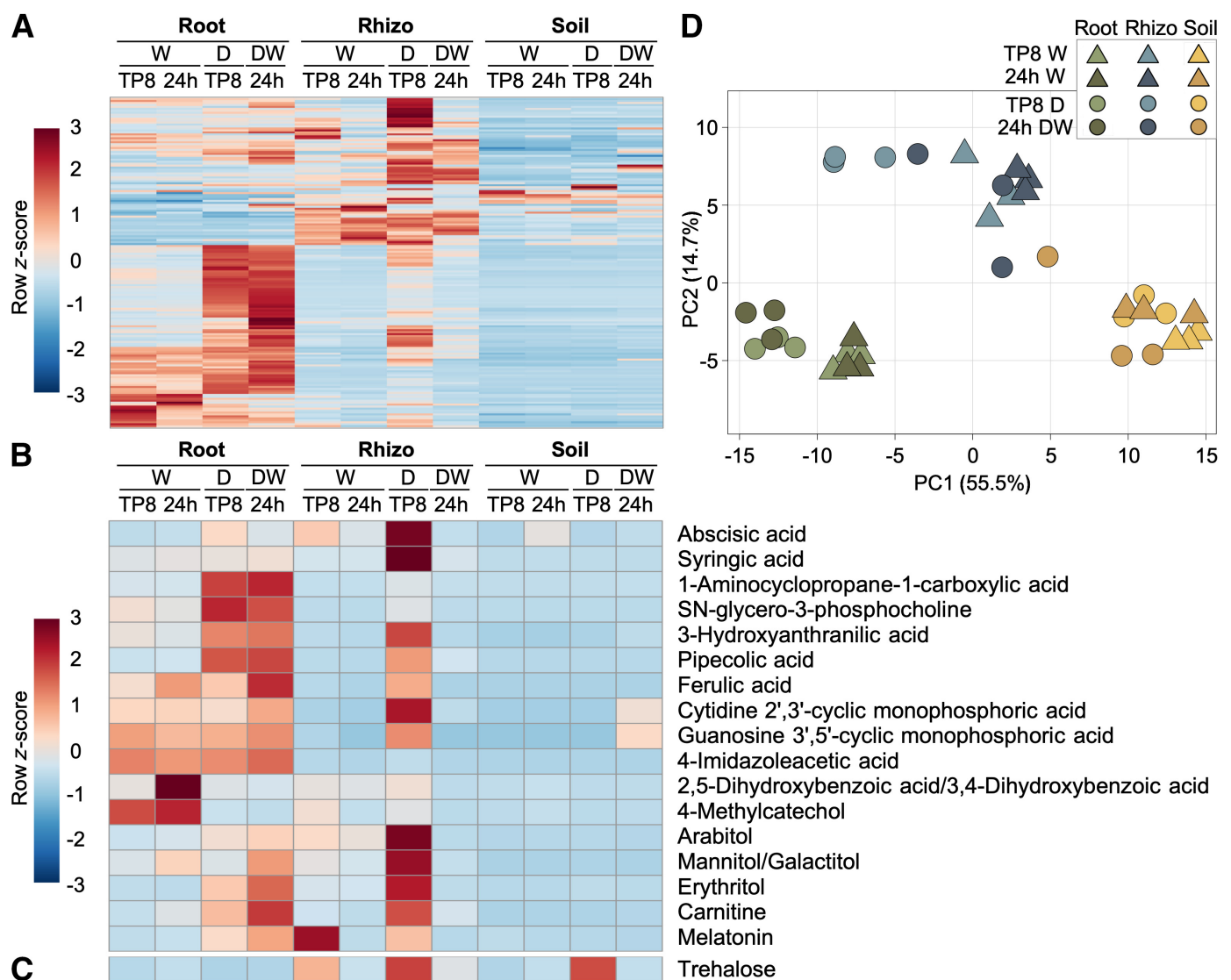

Fig. 3. Rewatering depletes rhizosphere metabolites following a prolonged drought. **A,** Heat map of relative peak heights of all observed metabolites ($n = 168$) across three compartments (roots, rhizosphere [rhizo], and soil), three treatments (watered [W], drought [D], and drought rewatered [DW]), and two time points (time point 8 [TP8] and 24 h later [24 h]). **B and C,** Heat map of the subset of metabolites that were depleted after rewatering (DW/D Log$_2$ fold change < -2, t test $P < 0.05$), with the predicted identity of metabolites listed beside each row. Note that all significant depletions were observed in the rhizosphere, B, except trehalose, C, which occurred in soil. **D,** Principal component analysis (PCA) plot of roots, rhizosphere, and soil metabolites.

data demonstrate that Pip application can stimulate in sorghum a classical phenotypic response observed in roots under stress.

As Pip is best known for its integral role as a component of the SAR systemic signaling pathway, we next explored the role of other components of the SAR pathway in modulating the root growth suppression phenotype. We utilized publicly available genetic resources in *Arabidopsis*, including *fmo-1*, *npr1-1*, *rbohd/rbohf*, and *azi1-2* mutants, which represent critical nodes in the SAR signaling pathway (Fig. 6), and measured the root growth of each of these validated *Arabidopsis* SAR mutants on media containing 1 mM Pip. Notably, mutants in FLAVIN-CONTAINING MONOOXYGENASE 1 (FMO-1), responsible for conversion of Pip to N-hydroxy-Pip (Hartmann et al. 2018; Fig. 6), displayed reduced root growth similar to the wild-type plant Col-0 in response to Pip (Fig. 6), indicating that the conversion of Pip by this enzyme is not needed to elicit reduced root growth. Likewise, mutants in NON EXPRESSER OF PATHOGENESIS RELATED GENES 1 (NPR1; Cao et al. 1994), an SA receptor required for SA-dependent SAR, and mutants in NADPH/RESPIRATORY BURST OXIDASE PROTEINS D and

F (RBOH D/F) and the lipid transfer protein AZELAIC ACID INDUCED 1 (AZI1; Jung et al. 2009; Wang et al. 2014), all of which are required for SA-independent SAR, also responded similarly to Col-0 (Fig. 6). Collectively, these results demonstrate that Pip-mediated suppression of root growth is independent of its role in the canonical immune-related SAR signaling pathway.

To further explore the relationship between Pip's enrichment during drought and its well-known role in SAR signaling, we examined the expression of genes involved in Pip catabolism during drought. There are two main pathways known to lead to Pip production in higher plants. One involves the enzymes ALD1 and SARD4, genes known to be indispensable for SAR-mediated immune response (Hartmann and Zeier 2018). The other pathway includes an LKR/SDH bifunctional enzyme, and this pathway has been observed to have increased expression under osmotic stress (Moulin et al. 2006), but is not required for pathogen-induced Pip production (Hartmann and Zeier 2018). Upon examining a root RNA-Seq dataset taken from plants grown in the same field and under the same experimental design as the main experiment (Varoquaux et al.
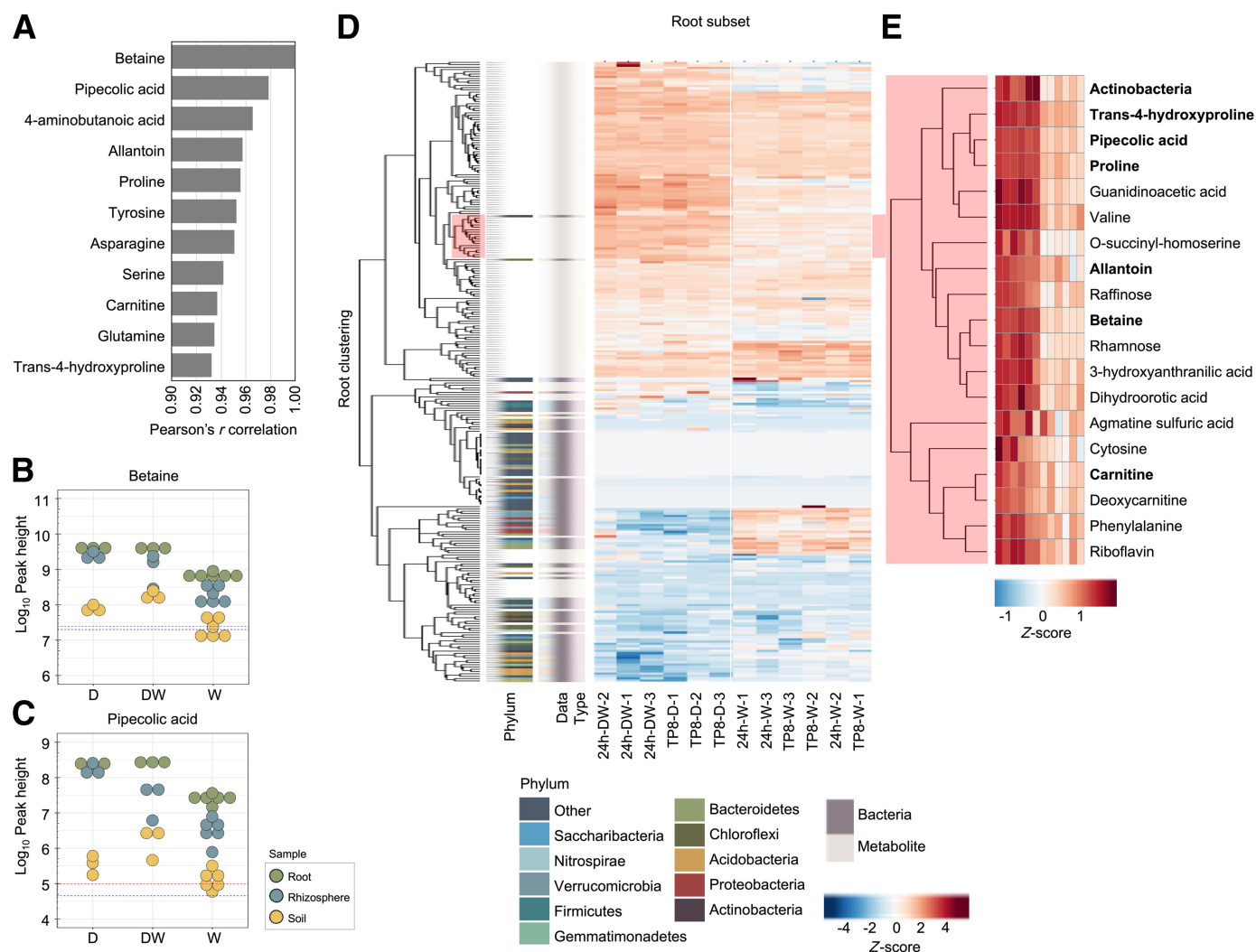

Fig. 4. Pipecolic acid abundance pattern mirrors drought markers. **A,** The top 10 metabolites correlated with the drought marker betaine across all sample types, treatments, and time points. **B and C,** $\log_{10}$ peak heights of individual metabolites. Each point represents an individual sample of roots (green), rhizosphere (blue), or soil (yellow). Dashed lines represent the limit of detection for individual metabolites, based on the average $\log_{10}$ peak heights of the sample blanks for roots (red) or rhizosphere and soil (blue). **D,** Heat map of relative abundances of all metabolites and bacteria amplicon sequence variants (grouped at the class level), clustered within the roots, across treatments (watered [W], drought [D], and drought rewatered [DW]) and time points (time point 8 [TP8] and 24 h later [24 h]). **E,** Zoom-in on Actinobacteria and closely clustering root metabolites, as highlighted in pink in D. Actinobacteria and the metabolites that are closely correlated with betaine (as in A) are in bold. Heat map values in D and E are matrix-wide z-scores.

2019), we observed that the LKR/SDH gene expression is significantly up-regulated in roots during drought stress compared with watered controls (Supplementary Fig. S2), whereas no significant increases in ALD1 and SARD4 expression are observed during drought (Supplementary Fig. S3). Collectively, these data provide additional evidence that the observed increases in Pip production are operating outside of its canonical role in immune signaling.

Pipecolic acid's role in the root microbiome. Next, we sought to determine if exogenous application of Pip could provoke changes in the root microbiome, specifically the abundance of Actinobacteria lineages, which show a correlation with Pip levels across compartment and treatment. To test this, we designed an experiment in which exogenously applied Pip was added to sorghum grown in Microbox containers inoculated with field soil. Sorghum seedlings were maintained in a growth chamber for 5 days, after which half of the Microboxes were subjected to either drought or watered conditions. One week later, plants were harvested. Shoot length was significantly shorter (Supplementary Fig. S4A) and

Fig. 5. Pipecolic acid reduces root growth. **A,** Root lengths of sterilized sorghum seedlings after 7 days of growth in water containing 0, 0.1, or 1 mM pipecolic acid (Pip). Different letters indicate significant differences in root length (ANOVA, Tukey-HSD, $P < 0.05$). This experiment was performed twice with similar results. **B,** Two representative seedlings from each treatment were photographed at the time of measurement. **C,** Root lengths of sterilized *Arabidopsis* seedlings after 10 days of growth in 1/2MS + 1% sucrose agar medium containing 0, 0.001, 0.01, 0.1, or 1 mM Pip. Different letters indicate significant differences in root length (ANOVA, Tukey-HSD, $P < 0.05$). Different colors represent plants from independent experiments ($n = 3$). **D,** One representative plate from each of 0- and 1-mM pipecolic acid treatments was photographed at the time of measurement.
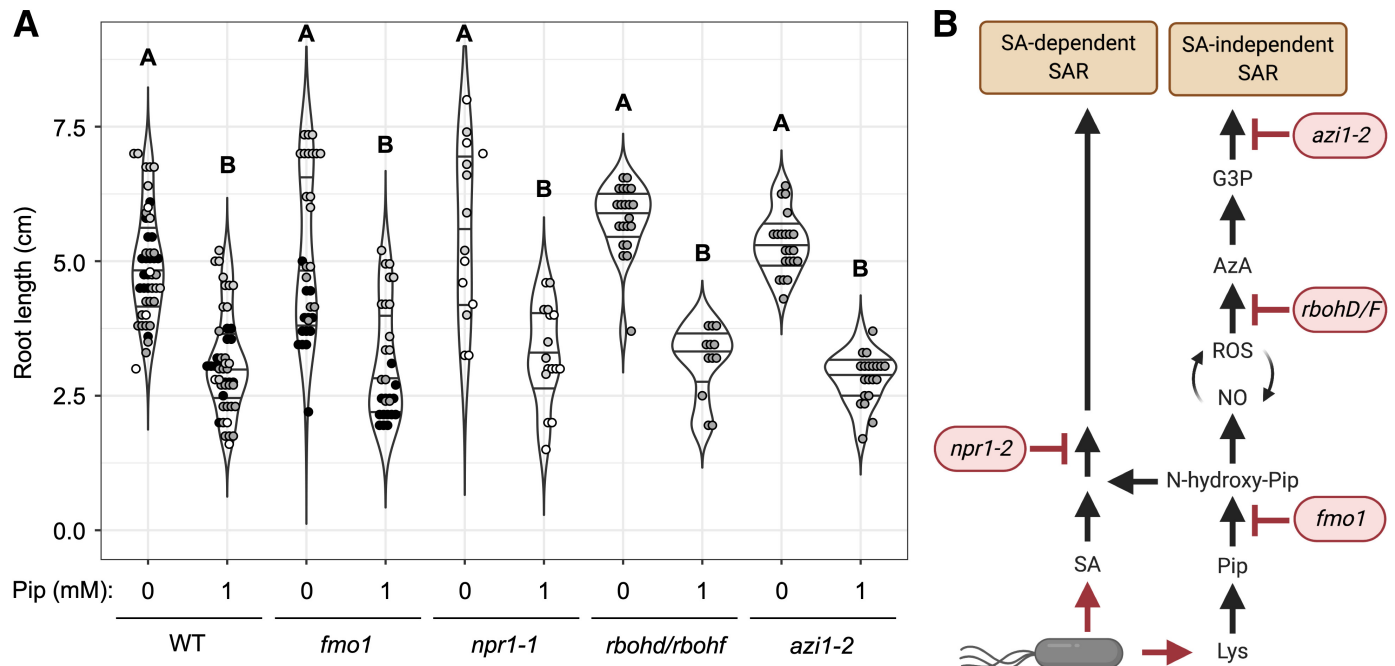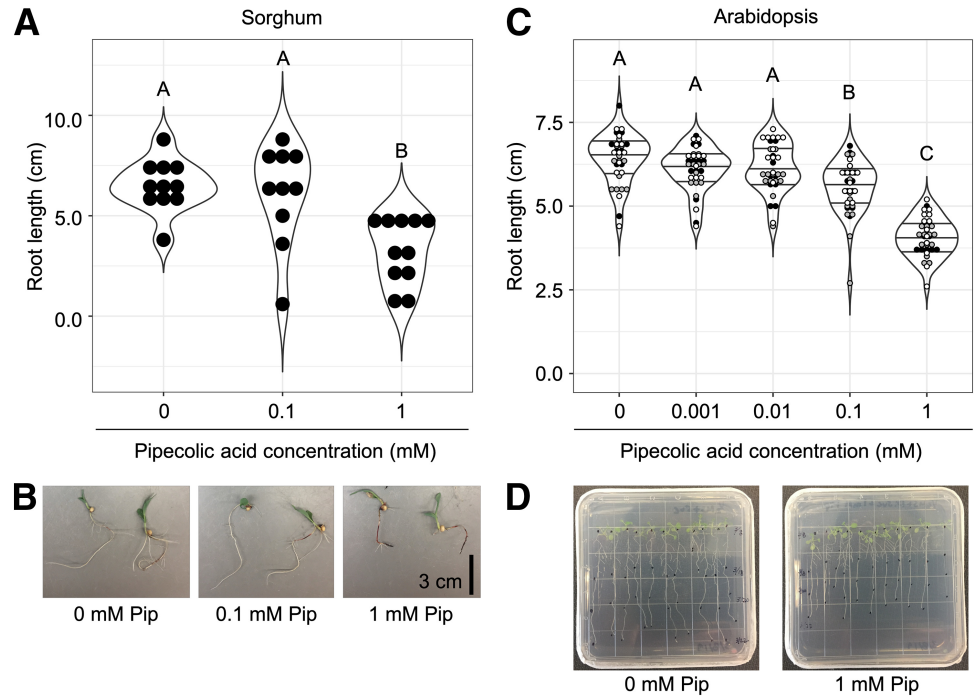

Fig. 6. Pipecolic acid root growth reduction is systemic acquired resistance (SAR)-independent. **A,** Root length of *Arabidopsis* Col-0 (WT) and *Arabidopsis* mutants grown on 1/2MS + 1% sucrose plates containing 0 or 1 mM Pip. Significance between treatments was evaluated by ANOVA with Tukey's HSD post hoc test ($P < 0.05$). Different colors represent plants from independent experiments. **B,** Simplified SAR pathway. Highlighted in red are the *Arabidopsis* mutants used to evaluate a potential interaction between SAR and Pip-mediated root growth suppression.

shoot fresh weight was significantly lower (Supplementary Fig. S4B) in drought-treated plants than in watered plants. Pip treatment did not significantly alter either shoot phenotype (Supplementary Fig. S4). To explore differences in the overall community composition of the root microbiomes of Pipecolic acid-treated plants from those of controls, we performed an ordination on Bray–Curtis distances between communities. PERMANOVA tests did not identify significant differences between Pip and control samples across the full experiment ($R^2 = 0.02$, $P = 0.417$), among droughted samples only ($R^2 = 0.039$, $P = 0.44$), or among watered samples only ($R^2 = 0.052$, $P = 0.19$). Samples were also ordinated using constrained analysis of principal coordinates (CAP). The observed separation in these ordinations based on Pip treatments from controls along the CAP2 axis, which explains 2% of the observed variation between sampled communities, was not statistically significant, indicating that Pip does not have an impact on overall community composition (Fig. 7A). To explore whether Pip influences the abundance of individual Actinobacterial taxa, differential abundance (DA) testing for differences between Pip-treated and control communities was performed. This analysis revealed 129
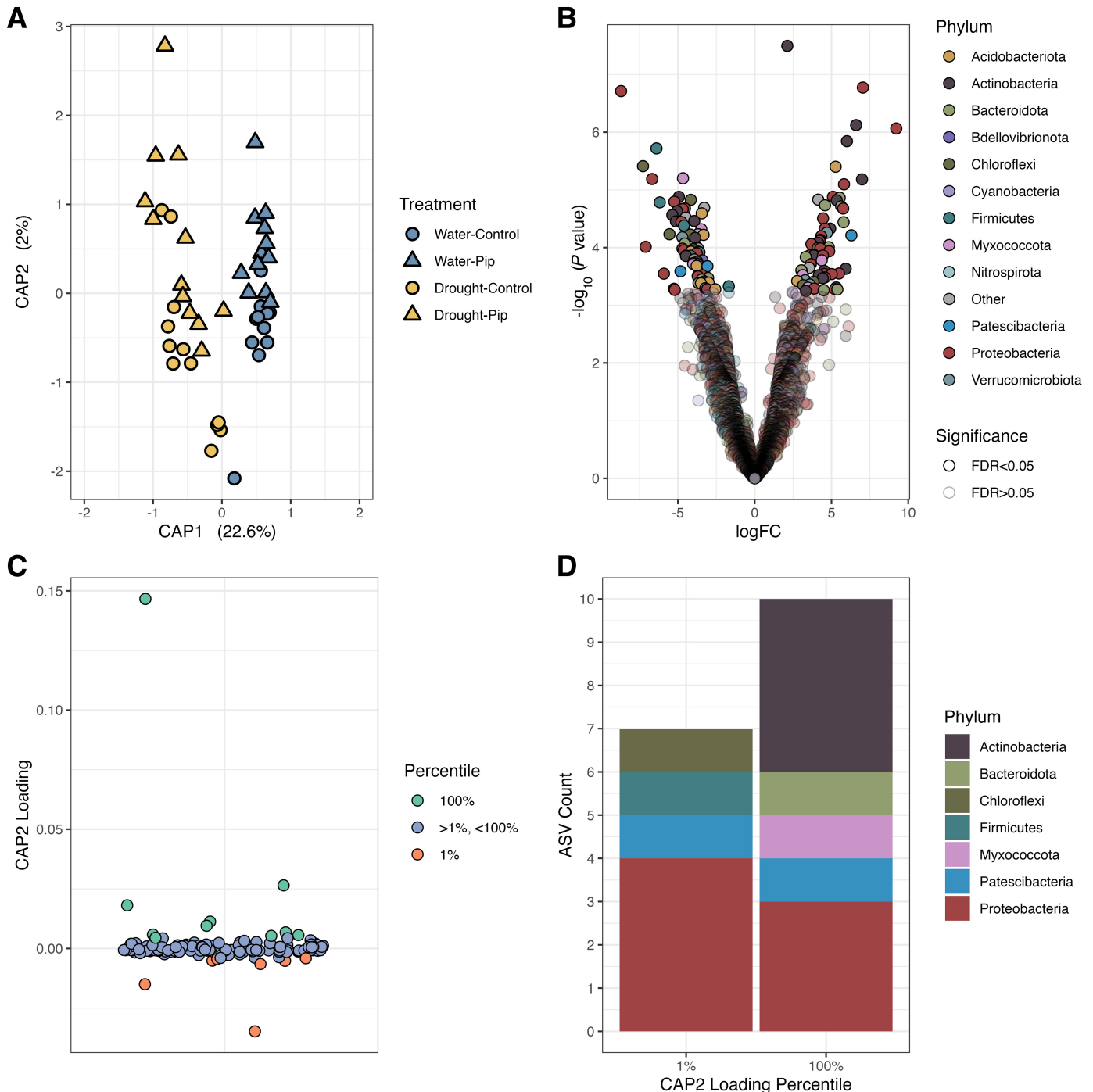

Fig. 7. Pipecolic acid treatment induces differential abundance of select taxa. **A,** Constrained analysis of principal coordinates (CAP) ordination of Microbox experiment. **B,** Differential abundance of amplicon sequence variants (ASVs) in a comparison of Pip-treated versus control samples. **C,** Significantly differentially abundant ASVs from B are plotted and colored according to their CAP2 score percentile ranks among all ASVs. **D,** Significantly differentially abundant ASVs that also fall into either 1 or 100% ranks of CAP2 score distributions.

significantly differentially abundant ASVs. Considering the separation of Pip-treated communities from controls along the CAP2 axis, each ASV was also labeled according to its percentile rank in the distribution of CAP2 scores (Fig. 7B) to identify ASVs with large effects on community separation by CAP2. Differentially abundant ASVs were plotted according to their CAP2 distribution (Fig. 7C), and ASVs that were both differentially abundant and falling into the 1% (control-associated) and 100% (Pip-associated) subsets of CAP2 loading scores were plotted by phylum (Fig. 7D). Among the ASVs identified as Pip-associated through this analysis, nearly half belonged to Actinobacteria ($n = 4$), whereas no Actinobacteria were identified as control-associated.

Finally, we explored the possibility that inclusion of pipecolic acid increased growth for Actinobacteria by serving as a carbon source. Seven isolates originally derived from sorghum roots, including both Actinobacteria and non-Actinobacteria, were grown on media containing moderate levels of pipecolic acid or a control carbon source (glucose) for a period of 14 days; none of the seven isolates chosen exhibited positive growth on Pip, suggesting that any influence pipecolic acid has on the abundance of these microbial taxa is not as a food source (Supplementary Fig. S5). Collectively, these results indicate that while exogenous Pip application does not alter overall rhizosphere microbiome composition, it may influence the abundances of individual Actinobacterial taxa, likely through indirect and as yet undetermined means.

DISCUSSION

Metabolite and microbial community compositions shift during drought and rewatering. Though the assemblage of the microbiome differs between roots, rhizosphere, and soil during drought, the underlying factors influencing these dissimilarities are not well understood. Plant metabolites and exudates have been hypothesized to play a role (Xu and Coleman-Derr 2019), but comprehensive studies of the global metabolite profiles across roots, rhizosphere, and soil have been hindered by the complexity of soil metabolite profiles. Advances in metabolomics have allowed characterization of metabolite profiles within and across complex substrates (You et al. 2019). Here, we collected both microbiome and metabolite profiles across three different compartments (sorghum roots, rhizosphere, and soil) and three treatments (watered, drought, and drought recovery). One of the primary observations was a general trend that many rhizosphere and root metabolites were more abundant during drought. This observation is in line with previous evidence that showed that root exudation by plants is increased during drought (Henry et al. 2007). Preece et al. (2018) showed oak trees to increase total organic carbon and root exudation (per gram of root biomass) by 21% in response to drought, and similar results have been observed in the grasses *Lolium perenne* and *Festuca arundinacea*, as well as the dicot *Medicago sativa* (Sanaullah et al. 2012). While these changes were observed to subside 6 weeks after a rewatering event, it was speculated that the large increase in released sugars during drought could significantly impact microbial community structure and overall biomass in the root environment (Preece et al. 2018). Indeed, one of the leading hypotheses for why plants increase carbon expenditure in response to stress is the recruitment of specific plant-growth-promoting microbial partners.

Analysis of the metabolomics data in this study also demonstrated that a large subset of the observed changes in metabolite abundance between drought and control are compartment-specific. While several of the best-studied metabolic indicators of drought, including both betaine and proline (Hare et al. 1999), appear to be strongly up-regulated in both roots and rhizosphere, others appear to be significantly enriched specifically in the roots. For instance, the metabolite serotonin, a compound speculated to play a role in abiotic stress response and ROS scavenging during abiotic stress (Kaur et al. 2015), shows strong up-regulation within root tissue but not rhizosphere. Lysine, well known as a metabolite whose concentration is altered by osmotic stress and which also serves as a precursor to pipecolic acid, similarly shows up-regulation in roots but not rhizosphere. In contrast to the patterns exhibited by these root-specific enrichments, others are most strongly enriched within the rhizosphere itself. One peculiar entry on this list is ABA, a phytohormone best known for its role in intercellular signaling within plant tissues during drought stress (Sah et al. 2016). Interestingly, past work has shown that ABA transporters located in root epidermal cells can efflux ABA into the rhizosphere (Hartung et al. 1996). This, in concert with the recent finding that specific microbes (including several Actinobacteria) can catabolize ABA as a sole carbon source (Belimov et al. 2014; Hasegawa et al. 1984), could suggest that ABA may serve in microbiome regulation outside of its normal role in hormone signaling. In addition to these drought-enriched compounds, we also observed a handful of drought-depleted metabolites, including two products related to immune functionality: 2,3-Dihydroxybenzoic acid is a major catabolic form of salicylic acid, and methylcatechol is a derivative of methyl salicylate, a major required component of systemic acquired immune signaling in plants (Cámara et al. 2007; Chen et al. 2019; Liu et al. 2011). Given the recent discovery of antagonism between drought responses and immunity (Moeder et al. 2010), it is perhaps unsurprising to see depletion of these compounds in root tissues exposed to decreased water availability. Collectively, these observations show that the root and rhizosphere metabolomes, like their microbiomes, can and do behave differently from one another, and highlight the importance of studying these compartments independently.

A previous study of sorghum roots and rhizosphere showed that bacterial community abundance reverts from Gram-positive dominance during drought to Gram-negative dominance in both compartments within a week following rewatering (Xu et al. 2018). In this study, we observed distinct patterns in the more immediate response of roots, rhizosphere, and soil microbiomes just 24 h after rewatering, with the rhizosphere being the most responsive. Interestingly, a similar result was observed in the metabolomics data, with the rhizosphere metabolite profile following rewatering exhibiting depletion in the majority of metabolites compared with the peak of drought. As the previous study lacked information relating to the rapid changes that occur after rewatering (Xu et al. 2018), the findings in this study provide context for how rapid shifts in the rhizosphere microbiome and metabolome following rewatering contribute to longer-term drought recovery. One possible explanation for these more rapid shifts observed in the rhizosphere may be that they are driven by flow of water, which can dilute root-adhering metabolites into the surrounding soil. Comparable studies on the temporal effects of drought and subsequent rewatering on metabolite profiles in grasses are lacking; however, previous studies of trees have reported mixed long-term effects. One study found that increases in exudation can be reversed following recovery from drought, to be indistinguishable from controls (Preece et al. 2018), while another found that extreme drought led to irreversible changes in exudation (Gargallo-Garriga et al. 2018). In the future, root metabolomics studies could benefit from selection of multiple time points following drought to understand the near- and long-term effects of drought in roots following rewatering.

Pipecolic acid-mediated root growth suppression is not mediated by the systemic acquired resistance pathway. In this study, we observed enrichment in many metabolites associated with drought, including those with well-defined functions in stress relief and those whose roles remain unclear. Of particular note, the

metabolite pipecolic acid was significantly enriched during drought, and its abundance correlated strongly with the highly enriched microbial marker of drought, the Actinobacteria, and the metabolites betaine, proline, and GABA. While Pip induction in response to osmotic stress has been noted in several previous studies (Goas et al. 1976; Moulin et al. 2006), by far Pip's best-known role is in systemic immune signaling in response to pathogens. Based on several lines of evidence, we propose that the observed Pip induction in this study likely falls outside of its known role in immune response. First, many recent studies in plants have shown that SA signaling and immune responses more generally are suppressed by drought (Ding et al. 2016; Yasuda et al. 2008). This phenomenon is primarily mediated through the drought-induced hormone ABA, which suppresses SA signaling (Ding et al. 2016). Indeed, a prior transcriptomic study in sorghum has shown that strong suppression of defense-related gene expression occurs in sorghum during drought (Varoquaux et al. 2019). Second, as further evidence that drought induction of Pip is operating independent of its known role in immune response (Schnake et al. 2020), we show using multiple previously validated *Arabidopsis* SAR pathway mutants that Pip's ability to suppress root growth acts independent of the established SAR signaling pathway. Finally, we provide transcriptomic evidence that the genetic pathway responsible for Pip enrichment under drought is one known to be dispensable for SAR signaling (Arruda and Barreto 2020). Collectively, these data support growing evidence from other plant systems (Kiyota et al. 2015; Moulin et al. 2006) that although Pip has been characterized as a component of SAR in plants, it may also act as a stress-responsive metabolite for other environmental shifts, including drought. It is worth noting that Pip's role as a signaling molecule in SAR has been evaluated primarily in leaves, leaving the door open for the possibility that Pip acts in different signaling pathways in a tissue-dependent manner.

Finally, we demonstrate that exogenous Pip application does not appear to impact overall root-associated microbiome composition, a result possibly impacted by the small sample size in the study or other experimental factors, including the failure of exogenous Pip application to reach relevant levels and localization of Pip induction during drought stress, or degradation of Pip across the duration of the experiment. However, it remains possible that drought-induced Pip accumulation in the root zone may contribute to the observed shifts in the root-associated microbiome by positively influencing the abundance of specific Actinobacteria. Among the actinobacterial lineages identified in this study as responding positively to Pip treatment is *Streptomyces*, one of the genera most strongly enriched by drought stress within the roots and rhizosphere (Fitzpatrick et al. 2018; Naylor et al. 2017; Santos-Medellín et al. 2017). This, along with the fact that no Actinobacteria lineages were identified as associated with the mock treatment, suggests that perhaps Pip induction could play a supportive role for other as yet unidentified factors that enrich for Gram-positives. It is worth noting that we find it unlikely that the impact of Pip completely explains changes observed under drought stress, as exogenous Pip application positively impacted the relative abundance of a number of other bacteria as well, across both Gram-positive and Gram-negative lineages. Additionally, we noted that members of the Firmicutes and Chloroflexi, Gram-positive lineages previously shown to have a tendency to drought enrichment in the root microbiome (Xu et al. 2018), both appeared to be negatively impacted by Pip treatment.

At present, the mechanism through which Pip could act to impact actinobacterial abundance patterns remains unclear, although we envision several possibilities. First, our results suggest that any such influence is unlikely to be as a direct carbon source, since none of the isolates tested showed significant growth on pipecolic acid. Instead, Pip may contribute to community dynamics by acting directly as a microbial osmoprotectant. In prior studies, Pip has been demonstrated to improve the growth of diverse bacteria challenged by NaCl-induced osmotic stress, including the Actinobacteria lineage *Brevibacterium ammoniagenes* (Gouesbet et al. 1992) and the Proteobacteria lineages *Escherichia coli* (Gouesbet et al. 1994), *Sinorhizobium meliloti* (Gouffi et al. 2000), and *Silicibacter pomeroyi* (Neshich et al. 2013). These data suggest that Pip can be functional as an osmoprotectant across a range of both Gram-positive and Gram-negative bacteria, which both fits with our observations from the exogenous Pipecolic acid microbiome experiments and supports the hypothesis that as an osmoprotectant Pip remains an unlikely primary driver of the observed drought-induced changes in the root microbiome, which heavily favor Gram-positives. As an alternative, Pip could also play a more indirect role, with its enrichment serving as an intermediary signal or stimulant to other plant processes that have a more direct role in shaping microbial abundance patterns. Several mechanisms have been put forward as potential links to Gram-positive enrichment under drought stress, including glycerol-3-phosphate, a glycolysis intermediate that becomes heavily enriched under osmotic stress (Xu and Coleman-Derr 2019; Xu et al. 2018). Drought-induced changes in iron metabolism within plant roots have also been proposed as being involved (Xu et al. 2021). If Pip does serve as an upstream signal in a systemic signaling pathway that responds to drought stress, a wide variety of downstream effects, both physiological and metabolic, could be important. Interestingly, another drought-induced metabolite identified in our study, trans-4-hydroxyproline, has also been discovered to play a role in systemic signaling in plants (Taylor et al. 2012). Collectively, the data in this study and recent work by others suggest that metabolic shifts in the roots and rhizosphere during drought may include some impactful and as yet poorly understood mechanisms of response.

In conclusion, drought stress represents a significant challenge to agriculture, and many environments across the planet are experiencing drought of increasing severity and frequency (Lesk et al. 2016; Schwalm et al. 2017). In addition to changes in agronomic practice and plant breeding for drought resilience, a successful multifaceted approach to improved drought response in crops will likely include the use of microbial partners that play roles in combating drought stress. Because of simple cultivation techniques, short generation times, and proven transformation methods, microbiome engineering represents an attractive strategy for short-term crop improvement in the face of climate change. A key challenge to implementing this approach, however, is maintaining persistence of applied microbes following engraftment, which likely arises in part because of inadequate understanding of the complex metabolic dynamics of the introduced ecosystem. In this study we help demonstrate that the root dynamically responds to its abiotic environment through its metabolite exudates and that these changes may have knock-on effects for the microbes in the rhizosphere. In the future, taking such dynamics into account will help ensure more predictable outcomes for microbiome-based methods of crop improvement.

ACKNOWLEDGMENTS

LITERATURE CITED

Arruda, P., and Barreto, P. 2020. Lysine catabolism through the saccharopine pathway: Enzymes and intermediates involved in plant responses to abiotic and biotic stress. Front. Plant Sci. 11:587.

Badri, D. V., Chaparro, J. M., Zhang, R., Shen, Q., and Vivanco, J. M. 2013. Application of natural blends of phytochemicals derived from the root exudates of Arabidopsis to the soil reveal that phenolic-related compounds predominantly modulate the soil microbiome. J. Biol. Chem. 288:4502-4512.

Baraniya, D., Nannipieri, P., Kublik, S., Vestergaard, G., Schloter, M., and Schöler, A. 2018. The impact of the diurnal cycle on the microbial transcriptome in the rhizosphere of barley. Microb. Ecol. 75:830-833.

Belimov, A. A., Dodd, I. C., Safronova, V. I., Dumova, V. A., Shaposhnikov, A. I., Ladatko, A. G., and Davies, W. J. 2014. Abscisic acid metabolizing rhizobacteria decrease ABA concentrations in planta and alter plant growth. Plant Physiol. Biochem. 74:84-91.

Bernsdorff, F., Döring, A.-C., Gruner, K., Schuck, S., Bräutigam, A., and Zeier, J. 2016. Pipecolic acid orchestrates plant systemic acquired resistance and defense priming via salicylic acid-dependent and -independent pathways. Plant Cell 28:102-129.

Bolyen, E., Rideout, J. R., Dillon, M. R., Bokulich, N. A., Abnet, C. C., Al-Ghalith, G. A., Alexander, H., Alm, E. J., Arumugam, M., Asnicar, F., Bai, Y., Bisanz, J. E., Bittinger, K., Brejnrod, A., Brislawn, C. J., Brown, C. T., Callahan, B. J., Caraballo-Rodríguez, A. M., Chase, J., Cope, E. K., Da Silva, R., Diener, C., Dorrestein, P. C., Douglas, G. M., Durall, D. M., Duvallet, C., Edwardson, C. F., Ernst, M., Estaki, M., Fouquier, J., Gauglitz, J. M., Gibbons, S. M., Gibson, D. L., Gonzalez, A., Gorlick, K., Guo, J., Hillmann, B., Holmes, S., Holste, H., Huttenhower, C., Huttley, G. A., Janssen, S., Jarmusch, A. K., Jiang, L., Kaehler, B. D., Kang, K. B., Keefe, C. R., Keim, P., Kelley, S. T., Knights, D., Koester, I., Kosciolek, T., Kreps, J., Langille, M. G. I., Lee, J., Ley, R., Liu, Y.-X., Loftfield, E., Lozupone, C., Maher, M., Marotz, C., Martin, B. D., McDonald, D., McIver, L. J., Melnik, A. V., Metcalf, J. L., Morgan, S. C., Morton, J. T., Naimey, A. T., Navas-Molina, J. A., Nothias, L. F., Orchanian, S. B., Pearson, T., Peoples, S. L., Petras, D., Preuss, M. L., Pruesse, E., Rasmussen, L. B., Rivers, A., Robeson, M. S., 2nd, Rosenthal, P., Segata, N., Shaffer, M., Shiffer, A., Sinha, R., Song, S. J., Spear, J. R., Swafford, A. D., Thompson, L. R., Torres, P. J., Trinh, P., Tripathi, A., Turnbaugh, P. J., Ul-Hasan, S., van der Hooft, J. J. J., Vargas, F., Vázquez-Baeza, Y., Vogtmann, E., von Hippel, M., Walters, W., Wan, Y., Wang, M., Warren, J., Weber, K. C., Williamson, C. H. D., Willis, A. D., Xu, Z. Z., Zaneveld, J. R., Zhang, Y., Zhu, Q., Knight, R., and Caporaso, J. G. 2019. Reproducible, interactive, scalable and extensible microbiome data science using QIIME 2. Nat. Biotechnol. 37:852-857.

Bowen, B. P., and Northen, T. R. 2010. Dealing with the unknown: Metabolomics and metabolite atlases. J. Am. Soc. Mass Spectrom. 21:1471-1476.

Bown, A. W., and Shelp, B. J. 2016. Plant GABA: Not just a metabolite. Trends Plant Sci. 21:811-813.

Bressan, M., Roncato, M.-A., Bellvert, F., Comte, G., Haichar, F. Z., Achouak, W., and Berge, O. 2009. Exogenous glucosinolate produced by Arabidopsis thaliana has an impact on microbes in the rhizosphere and plant roots. ISME J. 3:1243-1257.

Bulgarelli, D., Rott, M., Schlaeppi, K., Ver Loren van Themaat, E., Ahmadinejad, N., Assenza, F., Rauf, P., Huettel, B., Reinhardt, R., Schmelzer, E., Peplies, J., Gloeckner, F. O., Amann, R., Eickhorst, T., and Schulze-Lefert, P. 2012. Revealing structure and assembly cues for Arabidopsis root-inhabiting bacterial microbiota. Nature 488:91-95.

Caddell, D. F., Deng, S., and Coleman-Derr, D. 2019. Role of the plant root microbiome in abiotic stress tolerance. Pages 273-311 in: Seed Endophytes: Biology and Biotechnology. S. K. Verma and J. F. White, Jr., eds. Springer International Publishing, Cham, Switzerland.

Cai, T., Cai, W., Zhang, J., Zheng, H., Tsou, A. M., Xiao, L., Zhong, Z., and Zhu, J. 2009. Host legume-exuded antimetabolites optimize the symbiotic rhizosphere. Mol. Microbiol. 73:507-517.

Callahan, B. J., McMurdie, P. J., Rosen, M. J., Han, A. W., Johnson, A. J. A., and Holmes, S. P. 2016. DADA2: High-resolution sample inference from Illumina amplicon data. Nat. Methods 13:581-583.

Cámara, B., Bielecki, P., Kaminski, F., dos Santos, V. M., Plumeier, I., Nikodem, P., and Pieper, D. H. 2007. A gene cluster involved in degradation of substituted salicylates via ortho cleavage in Pseudomonas sp. strain MT1 encodes enzymes specifically adapted for transformation of 4-methylcatechol and 3-methylmuconate. J. Bacteriol. 189:1664-1674.

Cao, H., Bowling, S. A., Gordon, A. S., and Dong, X. 1994. Characterization of an Arabidopsis mutant that is nonresponsive to inducers of systemic acquired resistance. Plant Cell 6:1583-1592.

Cao, H., Glazebrook, J., Clarke, J. D., Volko, S., and Dong, X. 1997. The Arabidopsis NPR1 gene that controls systemic acquired resistance encodes a novel protein containing ankyrin repeats. Cell. 88:57-63.

Caspersen, S., Sundin, P., Munro, M., Aðalsteinsson, S., Hooker, J. E., and Jensén, P. 1999. Interactive effects of lettuce (Lactuca sativa L.), irradiance, and ferulic acid in axenic, hydroponic culture. Plant Soil 210:115-126.

Chaparro, J. M., Badri, D. V., Bakker, M. G., Sugiyama, A., Manter, D. K., and Vivanco, J. M. 2013. Root exudation of phytochemicals in Arabidopsis follows specific patterns that are developmentally programmed and correlate with soil microbial functions. PLoS One 8:e55731.

Chaparro, J. M., Badri, D. V., and Vivanco, J. M. 2014. Rhizosphere microbiome assemblage is affected by plant development. ISME J. 8:790-803.

Chen, L., Wang, W.-S., Wang, T., Meng, X.-F., Chen, T.-T., Huang, X.-X., Li, Y.-J., and Hou, B.-K. 2019. Methyl salicylate glucosylation regulates plant defense signaling and systemic acquired resistance. Plant Physiol. 180:2167-2181.

Chen, Y.-C., Holmes, E. C., Rajniak, J., Kim, J.-G., Tang, S., Fischer, C. R., Mudgett, M. B., and Sattely, E. S. 2018. N-hydroxy-pipecolic acid is a mobile metabolite that induces systemic disease resistance in Arabidopsis. Proc. Natl. Acad. Sci. U.S.A. 115:E4920-E4929.

Chong, J., Soufan, O., Li, C., Caraus, I., Li, S., Bourque, G., Wishart, D. S., and Xia, J. 2018. MetaboAnalyst 4.0: Towards more transparent and integrative metabolomics analysis. Nucleic Acids Res. 46:W486-W494.

Chong, J., Wishart, D. S., and Xia, J. 2019. Using MetaboAnalyst 4.0 for comprehensive and integrative metabolomics data analysis. Curr. Protoc. Bioinf. 68:e86.

Ding, Y., Dommel, M., and Mou, Z. 2016. Abscisic acid promotes proteasome-mediated degradation of the transcription coactivator NPR 1 in Arabidopsis thaliana. Plant J. 86:20-34.

Dixon, P. 2003. VEGAN, a package of R functions for community ecology. J. Veg. Sci. 14:927-930.

Edwards, J., Johnson, C., Santos-Medellín, C., Lurie, E., Podishetty, N. K., Bhatnagar, S., Eisen, J. A., and Sundaresan, V. 2015. Structure, variation, and assembly of the root-associated microbiomes of rice. Proc. Natl. Acad. Sci. U.S.A. 112:E911-E920.

Edwards, J. A., Santos-Medellín, C. M., Liechty, Z. S., Nguyen, B., Lurie, E., Eason, S., Phillips, G., and Sundaresan, V. 2018. Compositional shifts in root-associated bacterial and archaeal microbiota track the plant life cycle in field-grown rice. PLoS Biol. 16:e2003862.

Fàbregas, N., and Fernie, A. R. 2019. The metabolic response to drought. J. Exp. Bot. 70:1077-1085.

Fang, Y., and Xiong, L. 2015. General mechanisms of drought response and their application in drought resistance improvement in plants. Cell. Mol. Life Sci. 72:673-689.

Fitzpatrick, C. R., Copeland, J., Wang, P. W., Guttman, D. S., Kotanen, P. M., and Johnson, M. T. J. 2018. Assembly and ecological function of the root microbiome across angiosperm plant species. Proc. Natl. Acad. Sci. U.S.A. 115:E1157-E1165.

Gao, C., Montoya, L., Xu, L., Madera, M., Hollingsworth, J., Purdom, E., Singan, V., Vogel, J., Hutmacher, R. B., Dahlberg, J. A., Coleman-Derr, D., Lemaux, P. G., and Taylor, J. W. 2020. Fungal community assembly in drought-stressed sorghum shows stochasticity, selection, and universal ecological dynamics. Nat. Commun. 11:34.

Gargallo-Garriga, A., Preece, C., Sardans, J., Oravec, M., Urban, O., and Peñuelas, J. 2018. Root exudate metabolomes change under drought and show limited capacity for recovery. Sci. Rep. 8:12696.

Goas, G., Goas, M., and Larher, F. 1976. Formation de l'acide pipécolique chez Triglochin maritima. Can. J. Bot. 54:1221-1227.

Gouesbet, G., Blanco, C., Hamelin, J., and Bernard, T. 1992. Osmotic adjustment in Brevibacterium ammoniagenes: Pipecolic acid accumulation at elevated osmolalities. J. Gen. Microbiol. 138:959-965.

Gouesbet, G., Jebbar, M., Talibart, R., Bernard, T., and Blanco, C. 1994. Pipecolic acid is an osmoprotectant for Escherichia coli taken up by the general osmoporters ProU and ProP. Microbiology 140:2415-2422.

Gouffi, K., Bernard, T., and Blanco, C. 2000. Osmoprotection by pipecolic acid in Sinorhizobium meliloti: Specific effects of D and L isomers. Appl. Environ. Microbiol. 66:2358-2364.

Haney, C. H., Samuel, B. S., Bush, J., and Ausubel, F. M. 2015. Associations with rhizosphere bacteria can confer an adaptive advantage to plants. Nat. Plants 1:15051.

Hare, P., Cress, W. A., and van Staden, J. 1999. Proline synthesis and degradation: A model system for elucidating stress-related signal transduction. J. Exp. Bot. 50:413-434.

Hartmann, M., and Zeier, J. 2018. L-Lysine metabolism to N-hydroxypipecolic acid: An integral immune-activating pathway in plants. Plant J. 96:5-21.

Hartmann, M., Zeier, T., Bernsdorff, F., Reichel-Deland, V., Kim, D., Hohmann, M., Scholten, N., Schuck, S., Bräutigam, A., Hölzel, T., Ganter, C., and Zeier, J. 2018. Flavin monooxygenase-generated N-hydroxypipecolic acid is a critical element of plant systemic immunity. Cell. 173:456-469.e16.

Hartung, W., Sauter, A., Turner, N. C., Fillery, I., and Heilmeier, H. 1996. Abscisic acid in soils: What is its function and which factors and mechanisms influence its concentration? Plant Soil 184:105-110.

Hasegawa, S., Poling, S. M., Maier, V. P., and Bennett, R. D. 1984. Metabolism of abscisic acid: Bacterial conversion to dehydrovomifoliol and vomifoliol dehydrogenase activity. Phytochemistry 23:2769-2771.

Henry, A., Doucette, W., Norton, J., and Bugbee, B. 2007. Changes in crested wheatgrass root exudation caused by flood, drought, and nutrient stress. J. Environ. Qual. 36:904-912.

Hu, L., Robert, C. A. M., Cadot, S., Zhang, X., Ye, M., Li, B., Manzo, D., Chervet, N., Steinger, T., van der Heijden, M. G. A., Schlaeppi, K., and Erb, M. 2018. Root exudate metabolites drive plant–soil feedbacks on growth and defense by shaping the rhizosphere microbiota. Nat. Commun. 9:2738.

Huang, A. C., Jiang, T., Liu, Y.-X., Bai, Y.-C., Reed, J., Qu, B., Goossens, A., Nützmann, H.-W., Bai, Y., and Osbourn, A. 2019. A specialized metabolic network selectively modulates Arabidopsis root microbiota. Science 364:eaau6389.

Irani, S., and Todd, C. D. 2018. Exogenous allantoin increases Arabidopsis seedlings tolerance to NaCl stress and regulates expression of oxidative stress response genes. J. Plant Physiol. 221:43-50.

Iven, T., König, S., Singh, S., Braus-Stromeyer, S. A., Bischoff, M., Tietze, L. F., Braus, G. H., Lipka, V., Feussner, I., and Dröge-Laser, W. 2012. Transcriptional activation and production of tryptophan-derived secondary metabolites in Arabidopsis roots contributes to the defense against the fungal vascular pathogen Verticillium longisporum. Mol. Plant. 5:1389-1402.

Jung, H. W., Tschaplinski, T. J., Wang, L., Glazebrook, J., and Greenberg, J. T. 2009. Priming in systemic plant immunity. Science 324:89-91.

Kaur, H., Mukherjee, S., Baluska, F., and Bhatla, S. C. 2015. Regulatory roles of serotonin and melatonin in abiotic stress tolerance in plants. Plant Signal. Behav. 10:e1049788.

Khan, N., Bano, A., and Babar, M. A. 2019. Metabolic and physiological changes induced by plant growth regulators and plant growth promoting rhizobacteria and their impact on drought tolerance in Cicer arietinum L. PLoS One 14:e0213040.

Kiyota, E., Pena, I. A., and Arruda, P. 2015. The saccharopine pathway in seed development and stress response of maize. Plant Cell Environ. 38:2450-2461.

Kolde, R. 2019. pheatmap: Pretty Heatmaps (1.0.12) [R]. https://CRAN.R-project.org/package=pheatmap

Korenblum, E., Dong, Y., Szymanski, J., Panda, S., Jozwiak, A., Massalha, H., Meir, S., Rogachev, I., and Aharoni, A. 2020. Rhizosphere microbiome mediates systemic root metabolite exudation by root-to-root signaling. Proc. Natl. Acad. Sci. U.S.A. 117:3874-3883.

Koyama, A., Steinweg, M. J., Haddix, M. L., Dukes, J. S., and Wallenstein, M. D. 2018. Soil bacterial community responses to altered precipitation and temperature regimes in an old field grassland are mediated by plants. FEMS Microbiol. Ecol. 94:fix156.

Lamesch, P., Berardini, T. Z., Li, D., Swarbreck, D., Wilks, C., Sasidharan, R., Muller, R., Dreher, K., Alexander, D. L., Garcia-Hernandez, M., Karthikeyan, A. S., Lee, C. H., Nelson, W. D., Ploetz, L., Singh, S., Wensel, A., and Huala, E. 2012. The Arabidopsis Information Resource (TAIR): Improved gene annotation and new tools. Nucleic Acids Res. 40:D1202-D1210.

Lesk, C., Rowhani, P., and Ramankutty, N. 2016. Influence of extreme weather disasters on global crop production. Nature. 529:84-87.

Liu, P.-P., von Dahl, C. C., and Klessig, D. F. 2011. The extent to which methyl salicylate is required for signaling systemic acquired resistance is dependent on exposure to light after infection. Plant Physiol. 157:2216-2226.

Lundberg, D. S., Lebeis, S. L., Paredes, S. H., Yourstone, S., Gehring, J., Malfatti, S., Tremblay, J., Engelbrektson, A., Kunin, V., Del Rio, T. G., Edgar, R. C., Eickhorst, T., Ley, R. E., Hugenholtz, P., Tringe, S. G., and Dangl, J. L. 2012. Defining the core Arabidopsis thaliana root microbiome. Nature 488: 86-90.

McHardy, I. H., Goudarzi, M., Tong, M., Ruegger, P. M., Schwager, E., Weger, J. R., Graeber, T. G., Sonnenburg, J. L., Horvath, S., Huttenhower, C., McGovern, D. P., Fornace, A. J., Jr., Borneman, J., and Braun, J. 2013. Integrative analysis of the microbiome and metabolome of the human intestinal mucosal surface reveals exquisite inter-relationships. Microbiome 1:17.

McMurdie, P. J., and Holmes, S. 2013. phyloseq: An R package for reproducible interactive analysis and graphics of microbiome census data. PLoS One 8:e61217.

Mishina, T. E., and Zeier, J. 2006. The Arabidopsis flavin-dependent monooxygenase FMO1 is an essential component of biologically induced systemic acquired resistance. Plant Physiol. 141:1666-1675.

Moeder, W., Ung, H., Mosher, S., and Yoshioka, K. 2010. SA-ABA antagonism in defense responses. Plant Signal. Behav. 5:1231-1233.

Moulin, M., Deleu, C., Larher, F., and Bouchereau, A. 2006. The lysine-ketoglutarate reductase–accharopine dehydrogenase is involved in the osmo-induced synthesis of pipecolic acid in rapeseed leaf tissues. Plant Physiol. Biochem. 44:474-482.

Návarová, H., Bernsdorff, F., Döring, A.-C., and Zeier, J. 2012. Pipecolic acid, an endogenous mediator of defense amplification and priming, is a critical regulator of inducible plant immunity. Plant Cell 24:5123-5141.

Naylor, D., DeGraaf, S., Purdom, E., and Coleman-Derr, D. 2017. Drought and host selection influence bacterial community dynamics in the grass root microbiome. ISME J. 11:2691-2704.

Neshich, I. A. P., Kiyota, E., and Arruda, P. 2013. Genome-wide analysis of lysine catabolism in bacteria reveals new connections with osmotic stress resistance. ISME J. 7:2400-2410.

Nourimand, M., and Todd, C. D. 2017. Allantoin contributes to the stress response in cadmium-treated Arabidopsis roots. Plant Physiol. Biochem. 119:103-109.

Ofek-Lalzar, M., Sela, N., Goldman-Voronov, M., Green, S. J., Hadar, Y., and Minz, D. 2014. Niche and host-associated functional signatures of the root surface microbiome. Nat. Commun. 5:4950.

Oliveros, J. C. 2007-2015. Venny 2.1. An interactive tool for comparing lists with Venn's diagrams. https://bioinfogp.cnb.csic.es/tools/venny/index.html

Oney-Birol, S. 2019. Exogenous L-carnitine promotes plant growth and cell division by mitigating genotoxic damage of salt stress. Sci. Rep. 9: 17229.

Peiffer, J. A., Spor, A., Koren, O., Jin, Z., Tringe, S. G., Dangl, J. L., Buckler, E. S., and Ley, R. E. 2013. Diversity and heritability of the maize rhizosphere microbiome under field conditions. Proc. Natl. Acad. Sci. U.S.A. 110: 6548-6553.

Philip-Hollingsworth, S., Hollingsworth, R. I., and Dazzo, F. B. 1991. N-acetylglutamic acid: An extracellular nod signal of Rhizobium trifolii ANUS43 that induces root hair branching and nodule-like primordia in white clover roots. J. Biol. Chem. 266:16854-16858.

Preece, C., Farré-Armengol, G., Llusià, J., and Peñuelas, J. 2018. Thirsty tree roots exude more carbon. Tree Physiol. 38:690-695.

Quast, C., Pruesse, E., Yilmaz, P., Gerken, J., Schweer, T., Yarza, P., Peplies, J., and Glöckner, F. O. 2013. The SILVA ribosomal RNA gene database project: Improved data processing and web-based tools. Nucleic Acids Res. 41:D590-D596.

R Core Team. 2021. The R project for statistical computing. https://www.R-project.org/

Rai, V. K. 2002. Role of amino acids in plant responses to stresses. Biol. Plant. 45:481-487.

Ranieri, A., Bernardi, R., Lanese, P., and Soldatini, G. F. 1989. Changes in free amino acid content and protein pattern of maize seedlings under water stress. Environ. Exp. Bot. 29:351-357.

Robinson, M. D., McCarthy, D. J., and Smyth, G. K. 2010. edgeR: A bioconductor package for differential expression analysis of digital gene expression data. Bioinformatics 26:139-140.

Roux, P.-F., Oddos, T., and Stamatas, G. 2022. Deciphering the role of skin surface microbiome in skin health: An integrative multiomics approach reveals three distinct metabolite–microbe clusters. J. Invest. Dermatol. 142:469-479.e5.

Sah, S. K., Reddy, K. R., and Li, J. 2016. Abscisic acid and abiotic stress tolerance in crop plants. Front. Plant Sci. 7:571.

Sakamoto, A., and Murata, N. 2000. Genetic engineering of glycinebetaine synthesis in plants: Current status and implications for enhancement of stress tolerance. J. Exp. Bot. 51:81-88.

Sanaullah, M., Rumpel, C., Charrier, X., and Chabbi, A. 2012. How does drought stress influence the decomposition of plant litter with contrasting quality in a grassland ecosystem? Plant Soil 352:277-288.

Santos-Medellín, C., Edwards, J., Liechty, Z., Nguyen, B., and Sundaresan, V. 2017. Drought stress results in a compartment-specific restructuring of the rice root-associated microbiomes. mBio 8:e00764-17.

Schnake, A., Hartmann, M., Schreiber, S., Malik, J., Brahmann, L., Yildiz, I., von Dahlen, J., Rose, L. E., Scaffrath, U., and Zeier, J. 2020. Inducible biosynthesis and immune function of the systemic acquired resistance inducer N-hydroxypipecolic acid in monocotyledonous and dicotyledonous plants. J. Exp. Bot. 71:6444-6459.

Schneider, C. A., Rasband, W. S., and Eliceiri, K. W. 2012. NIH Image to ImageJ: 25 years of image analysis. Nat. Methods 9:671-675.

Schwalm, C. R., Anderegg, W. R. L., Michalak, A. M., Fisher, J. B., Biondi, F., Koch, G., Litvak, M., Ogle, K., Shaw, J. D., Wolf, A., Huntzinger, D. N., Schaefer, K., Cook, R., Wei, Y., Fang, Y., Hayes, D., Huang, M., Jain, A., and Tian, H. 2017. Global patterns of drought recovery. Nature 548: 202-205.

Sebastian, J., Yee, M.-C., Goudinho Viana, W., Rellán-Álvarez, R., Feldman, M., Priest, H. D., Trontin, C., Lee, T., Jiang, H., Baxter, I., Mockler, T. C., Hochholdinger, F., Brutnell, T. P., and Dinneny, J. R. 2016. Grasses suppress shoot-borne roots to conserve water during drought. Proc. Natl. Acad. Sci. U.S.A. 113:8861-8866.

Simmons, T., Caddell, D. F., Deng, S., and Coleman-Derr, D. 2018. Exploring the root microbiome: Extracting bacterial community data from the soil, rhizosphere, and root endosphere. J. Vis. Exp. 135:e57561.

Simmons, T., Styer, A. B., Pierroz, G., Gonçalves, A. P., Pasricha, R., Hazra, A. B., Bubner, P., and Coleman-Derr, D. 2020. Drought drives spatial variation in the millet root microbiome. Front. Plant Sci. 11:599.

Smith, C. A., O'Maille, G., Want, E. J., Qin, C., Trauger, S. A., Brandon, T. R., Custodio, D. E., Abagyan, R., and Siuzdak, G. 2005. METLIN: A metabolite mass spectral database. Ther. Drug Monit. 27:747-751.

Taylor, C. M., Karunaratne, C. V., and Xie, N. 2012. Glycosides of hydroxyproline: Some recent, unusual discoveries. Glycobiology 22:757-767.

Torres, M. A., Dangl, J. L., and Jones, J. D. G. 2002. *Arabidopsis* gp91[phox] homologues *AtrbohD* and *AtrbohF* are required for accumulation of reactive oxygen intermediates in the plant defense response. Proc. Natl. Acad. Sci. U.S.A. 99:517-522.

Tsuji, W., Inanaga, S., Araki, H., Morita, S., An, P., and Sonobe, K. 2005. Development and distribution of root system in two grain sorghum cultivars originated from Sudan under drought stress. Plant Prod. Sci. 8:553-562.

Varoquaux, N., Cole, B., Gao, C., Pierroz, G., Baker, C. R., Patel, D., Madera, M., Jeffers, T., Hollingsworth, J., Sievert, J., Yoshinaga, Y., Owiti, J. A., Singan, V. R., DeGraaf, S., Xu, L., Blow, M. J., Harrison, M. J., Visel, A., Jansson, C., Niyogi, K. K., Hutmacher, R., Coleman-Derr, D., O'Malley, R. C., Taylor, J. W., Dahlberg, J., Vogel, J. P., Lemaux, P. G., and Purdom, E. 2019. Transcriptomic analysis of field-droughted sorghum from seedling to maturity reveals biotic and metabolic responses. Proc. Natl. Acad. Sci. U.S.A. 116:27124-27132.

Walitang, D. I., Kim, C.-G., Kim, K., Kang, Y., Kim, Y. K., and Sa, T. 2018. The influence of host genotype and salt stress on the seed endophytic community of salt-sensitive and salt-tolerant rice cultivars. BMC Plant Biol. 18:51.

Wallace, J. G., Kremling, K. A., Kovar, L. L., and Buckler, E. S. 2018. Quantitative genetics of the maize leaf microbiome. Phytobiomes J. 2:208-224.

Wang, C., El-Shetehy, M., Shine, M. B., Yu, K., Navarre, D., Wendehenne, D., Kachroo, A., and Kachroo, P. 2014. Free radicals mediate systemic acquired resistance. Cell Rep. 7:348-355.

Wang, C., Liu, R., Lim, G.-H., de Lorenzo, L., Yu, K., Zhang, K., Hunt, A. G., Kachroo, A., and Kachroo, P. 2018a. Pipecolic acid confers systemic immunity by regulating free radicals. Sci. Adv. 4:eaar4509.

Wang, D., Tang, G., Wang, Y., Yu, J., Chen, L., Chen, J., Wu, Y., Zhang, Y., Cao, Y., and Yao, J. 2023. Rumen bacterial cluster identification and its influence on rumen metabolites and growth performance of young goats. Anim. Nutr. 15:34-44.

Wang, Y., Bouwmeester, K., van de Mortel, J. E., Shan, W., and Govers, F. 2013. A novel Arabidopsis–oomycete pathosystem: Differential interactions with *Phytophthora capsici* reveal a role for camalexin, indole glucosinolates and salicylic acid in defence. Plant Cell Environ. 36:1192-1203.

Wang, Y., Schuck, S., Wu, J., Yang, P., Döring, A.-C., Zeier, J., and Tsuda, K. 2018b. A MPK3/6–WRKY33–ALD1–pipecolic acid regulatory loop contributes to systemic acquired resistance. Plant Cell 30:2480-2494.

Wang, Z., Zhang, J., Wu, F., and Zhou, X. 2018c. Changes in rhizosphere microbial communities in potted cucumber seedlings treated with syringic acid. PLoS One 13:e0200007.

Xu, L., and Coleman-Derr, D. 2019. Causes and consequences of a conserved bacterial root microbiome response to drought stress. Curr. Opin. Microbiol. 49:1-6.

Xu, L., Dong, Z., Chiniquy, D., Pierroz, G., Deng, S., Gao, C., Diamond, S., Simmons, T., Wipf, H. M.-L., Caddell, D., Varoquaux, N., Madera, M. A., Hutmacher, R., Deutschbauer, A., Dahlberg, J. A., Guerinot, M. L., Purdom, E., Banfield, J. F., Taylor, J. W., Lemaux, P. G., and Coleman-Derr, D. 2021. Genome-resolved metagenomics reveals role of iron metabolism in drought-induced rhizosphere microbiome dynamics. Nat. Commun. 12:3209.

Xu, L., Naylor, D., Dong, Z., Simmons, T., Pierroz, G., Hixson, K. K., Kim, Y.-M., Zink, E. M., Engbrecht, K. M., Wang, Y., Gao, C., DeGraaf, S., Madera, M. A., Sievert, J. A., Hollingsworth, J., Birdseye, D., Scheller, H. V., Hutmacher, R., Dahlberg, J., Jansson, C., Taylor, J. W., Lemaux, P. G., and Coleman-Derr, D. 2018. Drought delays development of the sorghum root microbiome and enriches for monoderm bacteria. Proc. Natl. Acad. Sci. U.S.A. 115:E4284-E4293.

Yao, Y., Sun, T., Wang, T., Ruebel, O., Northen, T., and Bowen, B. P. 2015. Analysis of metabolomics datasets with high-performance computing and metabolite atlases. Metabolites. 5:431-442.

Yasuda, M., Ishikawa, A., Jikumaru, Y., Seki, M., Umezawa, T., Asami, T., Maruyama-Nakashita, A., Kudo, T., Shinozaki, K., Yoshida, S., and Nakashita, H. 2008. Antagonistic interaction between systemic acquired resistance and the abscisic acid-mediated abiotic stress response in *Arabidopsis*. Plant Cell 20:1678-1692.

You, J., Zhang, Y., Liu, A., Li, D., Wang, X., Dossa, K., Zhou, R., Yu, J., Zhang, Y., Wang, L., and Zhang, X. 2019. Transcriptomic and metabolomic profiling of drought-tolerant and susceptible sesame genotypes in response to drought stress. BMC Plant Biol. 19:267.

Zhalnina, K., Louie, K. B., Hao, Z., Mansoori, N., da Rocha, U. N., Shi, S., Cho, H., Karaoz, U., Loqué, D., Bowen, B. P., Firestone, M. K., Northen, T. R., and Brodie, E. L. 2018. Dynamic root exudate chemistry and microbial substrate preferences drive patterns in rhizosphere microbial community assembly. Nat. Microbiol. 3:470-480.

Zhang, K., Halitschke, R., Yin, C., Liu, C.-J., and Gan, S.-S. 2013. Salicylic acid 3-hydroxylase regulates *Arabidopsis* leaf longevity by mediating salicylic acid catabolism. Proc. Natl. Acad. Sci. U.S.A. 110:14807-14812.

Zhang, N., Wang, D., Liu, Y., Li, S., Shen, Q., and Zhang, R. 2014. Effects of different plant root exudates and their organic acid components on chemotaxis, biofilm formation and colonization by beneficial rhizosphere-associated bacterial strains. Plant Soil 374:689-700.